

Study of chiral symmetry restoration in linear and nonlinear $O(N)$ models using the auxiliary-field method

Elina Seel^a, Stefan Strüber^a, Francesco Giacosa^a, and Dirk H. Rischke^{a,b}

^a*Institute for Theoretical Physics, Goethe University,*

Max-von-Laue-Str. 1, D-60438 Frankfurt am Main, Germany and

^b*Frankfurt Institute for Advanced Studies, Goethe University,*
Ruth-Moufang-Str. 1, D-60438 Frankfurt am Main, Germany

We consider the $O(N)$ linear σ model and introduce an auxiliary field to eliminate the scalar self-interaction. Using a suitable limiting process this model can be continuously transformed into the nonlinear version of the $O(N)$ model. We demonstrate that, up to two-loop order in the CJT formalism, the effective potential of the model with auxiliary field is identical to the one of the standard $O(N)$ linear σ model, if the auxiliary field is eliminated using the stationary values for the corresponding one- and two-point functions. We numerically compute the chiral condensate and the σ - and π -meson masses at nonzero temperature in the one-loop approximation of the CJT formalism. The order of the chiral phase transition depends sensitively on the choice of the renormalization scheme. In the linear version of the model and for explicitly broken chiral symmetry, it turns from crossover to first order as the mass of the σ particle increases. In the nonlinear case, the order of the phase transition turns out to be of first order. In the region where the parameter space of the model allows for physical solutions, Goldstone's theorem is always fulfilled.

I. INTRODUCTION

Scalar models in $d + 1$ space-time dimensions with orthogonal symmetry are widely used in many areas of physics. Some applications of these $O(N)$ models are quantum dots, high-temperature superconductivity, low-dimensional systems, polymers, organic metals, biological molecular arrays, and chains. In this paper, we focus on a physical system consisting of interacting pions and σ mesons at nonzero temperature T . For three spatial dimensions, $d = 3$, an analytical solution to this model does not exist. Thus, one has to use many-body approximation schemes in order to compute quantities of interest, such as the effective potential, the order parameter, and the masses of the particles as a function of T . As an approximation scheme never gives the exact solution, it is of interest to compare different schemes and assess their physical relevance.

For $N = 4$ the $O(N)$ symmetry group for the internal degrees of freedom is locally isomorphic to the chiral $SU(2)_R \times SU(2)_L$ symmetry group of quantum chromodynamics (QCD) with $N_f = 2$ massless quark flavors. The phenomena of low-energy QCD are largely governed by chiral symmetry.

In the case of zero quark masses the QCD Lagrangian is invariant under $U(N_f)_R \times U(N_f)_L$ transformations, N_f being the number of quark flavors. However, the true symmetry of QCD is only $U(N_f)_V \times SU(N_f)_A$, because of the axial anomaly which explicitly breaks $U(1)_A$ due nontrivial topological effects [1]. For N_f nonzero but degenerate quark masses, the $SU(N_f)_A$ symmetry is explicitly broken, such that QCD has only a $U(N_f)_V$ flavor symmetry. In reality, different quark flavors have different masses, reducing the symmetry of QCD to $U(1)_V$, which corresponds to baryon number conservation. In the vacuum, the axial $SU(N_f)_A$ symmetry is also spontaneously broken by a non-vanishing expectation value of the quark condensate $\langle q\bar{q} \rangle \neq 0$ [2]. According to Goldstone's theorem, this leads to $N_f^2 - 1$ Goldstone bosons.

The chiral symmetry is restored at a temperature T which for dimensional reasons is expected to be of the order of $\Lambda_{QCD} \sim 200$ MeV. This scenario is indeed confirmed by lattice simulations, in which (for physical quark masses) a crossover transition at $T_c \sim 150$ MeV has been observed [3].

For vanishing quark masses, the high- and the low-temperature phases of QCD have different symmetries, and therefore must be separated by a phase transition. The order of this chiral phase transition is determined by the global symmetry of the QCD Lagrangian; for $U(N_f)_V \times U(N_f)_A$, the transition is of first order if $N_f \geq 2$; for $U(N_f)_V \times SU(N_f)_A$ the transition can be of second order if $N_f \leq 2$ [4]. If the quark masses are nonzero, the second-order phase transition becomes crossover.

The calculation of hadronic properties at nonzero temperature faces serious technical difficulties. For a nonconvex effective potential standard perturbation theory cannot be applied. Furthermore, nonzero temperature introduces an additional scale which invalidates the usual power counting in terms of the coupling constant [5]. A consistent calculation to a given order in the coupling constant then may require a resummation of whole classes of diagrams [6].

A convenient technique to perform such a resummation and thus arrive at a particular many-body approximation scheme is the so-called two-particle irreducible (2PI) or Cornwall-Jackiw-Tomboulis (CJT) formalism [7, 8], which

is a relativistic generalization of the Φ -functional formalism [9, 10]. The CJT formalism extends the concept of the generating functional $\Gamma[\phi]$ for one-particle irreducible (1PI) Green's functions to that for 2PI Green's functions $\Gamma[\phi, G]$, where ϕ and G are the one- and two-point functions. The central quantity in this formalism is the sum of all 2PI vacuum diagrams, $\Gamma_2[\phi, G]$. Any many-body approximation scheme can be derived as a particular truncation of $\Gamma_2[\phi, G]$.

An advantage of the CJT formalism is that it avoids double counting and fulfills detailed balance relations and thus is thermodynamically consistent. Another advantage is that the Noether currents are conserved for an arbitrary truncation of Γ_2 , as long as the one- and two-point functions transform as rank-1 and rank-2 tensors. A disadvantage is that Ward-Takahashi identities for higher-order vertex functions are no longer fulfilled [11]. As a consequence, Goldstone's theorem is violated [12, 13]. A strategy to restore Goldstone's theorem is to perform a so-called "external" resummation of random-phase approximation diagrams with internal lines given by the full propagators of the approximation used in the CJT formalism [11].

In the literature different many-body approximations have been applied to examine the thermodynamical behavior of the $O(N)$ model in its linear and nonlinear versions. In Ref. [14] optimized perturbation theory was used to compute the effective potential, spectral functions, and dilepton emission rates. The CJT formalism has been applied to study the thermodynamics of the $O(N)$ model in the so-called "double-bubble" approximation [12, 13, 15–24], in Ref. [25] sunset-type diagrams have been included. The $1/N$ expansion has also been used several times to study various properties of the $O(N)$ model at zero [26, 27] and nonzero [28–31] temperature.

In this paper, we derive the effective potential for the $O(N)$ linear σ model within the auxiliary-field method [32–34]. The auxiliary field allows us to obtain the nonlinear version of the σ model by a well-defined limiting process from the linear version. We demonstrate that, to two-loop order, the effective potential is equivalent to the one of the standard $O(N)$ linear σ model without auxiliary field, once the one- and two-point functions involving the auxiliary field are replaced by their stationary values. We then calculate the masses and the condensates of the $O(N)$ model at nonzero T in one-loop approximation. Although we restrict our treatment to one-loop order, the condensate equation for the auxiliary field introduces self-consistently computed loops in the equations for the masses. Therefore, the one-loop approximation with auxiliary field is qualitatively similar to the standard double-bubble (Hartree-Fock) approximation in the treatment without auxiliary field. However, since the equations for the masses differ quantitatively, they lead to different results for the order parameter and the masses of the particles as a function of T .

The order of the chiral phase transition depends sensitively on the choice of renormalization scheme. In the linear version of the model and for explicitly broken chiral symmetry, it turns from crossover to first order as the mass of the σ particle increases. In the counter-term renormalization scheme, this transition happens for smaller values of the σ meson than in the case where vacuum contributions to tadpole diagrams are simply neglected (the so-called trivial regularization). In the nonlinear case the phase transition is of first order. Besides, in the region where the parameter space of the model allows for physical solutions of the mass equations, Goldstone's theorem is always respected.

The manuscript is organized as follows: in Sec. II the linear and nonlinear versions of the model are presented and it is shown how they can be related with the help of an auxiliary field. In Sec. III the effective potential and the equations for the condensate and masses are derived. We demonstrate the equivalence of the auxiliary-field method to that of the standard approach (i.e., without auxiliary field) when replacing the one- and two-point functions of the auxiliary field by their stationary values. In Sec. IV the results are presented for the linear and nonlinear versions of the model in the case of non-vanishing and vanishing explicit symmetry breaking. Section V concludes this paper with a summary of our results and an outlook for further studies. An Appendix contains an alternative proof of the equivalence of the treatment with and without auxiliary field, and details concerning the renormalization of tadpole integrals.

We use units $\hbar = c = k_B = 1$. The metric tensor is $g^{\mu\nu} = \text{diag}(1, -1, -1, -1)$. Four-vectors are denoted by capital letters, $K^\mu = (k_0, \vec{k})$. We use the imaginary-time formalism to compute quantities at nonzero temperature, i.e., the energy is $k_0 = i\omega_n$, where ω_n is the Matsubara frequency. For bosons, $\omega_n = 2\pi nT$. Energy-momentum integrals are denoted as

$$\int_K f(K) \equiv T \sum_{n=-\infty}^{\infty} \int \frac{d^3\vec{k}}{(2\pi)^3} f(i\omega_n, \vec{k}). \quad (1)$$

II. THE $O(N)$ MODEL

The generating functional of the σ model with $O(N)$ symmetry at nonzero temperature T is given by

$$Z_L(\varepsilon, h) = \mathcal{N} \int \mathcal{D}\alpha \mathcal{D}\Phi \exp \left(\int_0^{1/T} d\tau \int_V d^3\vec{x} \mathcal{L}_{\sigma-\alpha} \right), \quad (2)$$

with the Lagrangian

$$\mathcal{L}_{\sigma-\alpha} = \frac{1}{2} (\partial_\mu \Phi)^2 - U(\Phi, \alpha) \quad , \quad U(\Phi, \alpha) = \frac{i}{2} \alpha (\Phi^2 - v_0^2) + \frac{N\varepsilon}{8} \alpha^2 - h\sigma \quad , \quad (3)$$

where $\Phi^2 = \Phi^t \Phi$, $\Phi^t = (\sigma, \pi_1, \dots, \pi_{N-1})$ and α is an auxiliary field serving as a Lagrange multiplier. One can obtain the generating functional of the $O(N)$ model in its familiar form by integrating out the field α :

$$Z_L(\varepsilon, h) = \tilde{\mathcal{N}} \int \mathcal{D}\Phi \exp \left(\int_0^{1/T} d\tau \int_V d^3\vec{x} \mathcal{L}_\sigma \right) \quad , \quad (4)$$

with the Lagrangian

$$\mathcal{L}_\sigma = \frac{1}{2} (\partial_\mu \Phi)^2 - \frac{1}{2N\varepsilon} (\Phi^2 - v_0^2)^2 + h\sigma \quad . \quad (5)$$

As one can see, the potential of the model exhibits the typical tilted Mexican-hat shape, with the parameter $1/\varepsilon$ being the coupling constant, h the parameter for explicit symmetry breaking, and v_0 the vacuum expectation value (v.e.v.) of Φ . The π_i fields can be identified as the pseudo-Goldstone fluctuations.

Another way to see the equivalence to the standard form of the $O(N)$ model is to use the equation of motion for the auxiliary field α ,

$$\frac{\delta \mathcal{L}_{\sigma-\alpha}}{\delta \alpha} - \partial_\mu \frac{\delta \mathcal{L}_{\sigma-\alpha}}{\delta \partial_\mu \alpha} = 0 \quad \implies \quad i\alpha = \frac{2}{N\varepsilon} (\Phi^2 - v_0^2) \quad . \quad (6)$$

When plugging the latter into $\mathcal{L}_{\sigma-\alpha}$ one recovers, as expected, the familiar Lagrangian \mathcal{L}_σ .

The advantage of the representation (2) of the generating functional of the *linear* σ model is that, by taking the limit $\varepsilon \rightarrow 0^+$, one naturally obtains the *nonlinear* version of the σ model with the fields constrained by the condition $\Phi^2 = v_0^2$. In fact,

$$\begin{aligned} Z_{NL}(h) &= \lim_{\varepsilon \rightarrow 0^+} Z_L(\varepsilon, h) = \lim_{\varepsilon \rightarrow 0^+} \mathcal{N} \int \mathcal{D}\alpha \mathcal{D}\Phi \exp \left[\int_0^{1/T} d\tau \int_V d^3\vec{x} \mathcal{L}_{\sigma-\alpha} \right] \\ &= \mathcal{N}' \int \mathcal{D}\Phi \delta[\Phi^2 - v_0^2] \exp \left\{ \int_0^{1/T} d\tau \int_V d^3\vec{x} \left[\frac{1}{2} (\partial_\mu \Phi)^2 + h\sigma \right] \right\} \quad , \end{aligned} \quad (7)$$

because $\delta[\Phi^2 - v_0^2]$ can be identified with

$$\delta[\Phi^2 - v_0^2] \sim \lim_{\varepsilon \rightarrow 0^+} \int \mathcal{D}\alpha \exp \left\{ - \int_0^{1/T} d\tau \int_V d^3\vec{x} \left[\frac{i}{2} \alpha (\Phi^2 - v_0^2) + \frac{N\varepsilon}{8} \alpha^2 \right] \right\} \quad , \quad (8)$$

which is the mathematically well-defined (i.e., convergent) form of the usual representation of the functional δ -function. Equation (8) ensures that the Mexican hat potential becomes infinitely steep and, consequently, the mass of the radial degree of freedom infinite.

Note that in some previous studies of the $O(N)$ nonlinear σ model [28, 29], the ε -dependence in Eq. (8) was not appropriately handled: there, the limit $\varepsilon \rightarrow 0^+$ was exchanged with the functional $\mathcal{D}\alpha$ integration, effectively setting $\varepsilon = 0$ in the exponent. This, however, is incorrect, since the additional term $\sim \varepsilon \alpha^2$ is essential to establish the link between the linear model and the nonlinear one. Without this term, an integration over the auxiliary field does not give the correct potential of the linear model. Thus, for a proper construction of the nonlinear limit of the $O(N)$ model the ε -dependence must be included.

III. THE CJT EFFECTIVE POTENTIAL

In this work we study the thermodynamical behavior of the $O(N)$ linear σ model, and in particular the temperature dependence of the masses of the modes and of the condensate. To this end one has to apply methods that go beyond the standard loop expansion which is not applicable when the effective potential is not convex [35], as is the case here because of spontaneous chiral symmetry breaking. A method that allows to compute quantities like the effective potential, the masses, and the order parameter at nonzero temperature is provided by the Cornwall-Jackiw-Tomboulis (CJT) formalism [7]. In order to apply this method, we need to identify the tree-level potential, the tree-level propagators, as well as the interaction vertices from the underlying Lagrangian.

A. Tree-level potential, tree-level propagators, and vertices

In our case, the fields occurring in the Lagrangian are $\sigma, \boldsymbol{\pi} \equiv (\pi_1, \dots, \pi_{N-1})^t$, as well as the auxiliary field α . In general, the fields σ and α attain non-vanishing vacuum expectation values. In order to take this fact into account, we perform a shift $\sigma \rightarrow \phi + \sigma$ and $\alpha \rightarrow \alpha_0 + \alpha$, respectively. This leaves the kinetic terms in the Lagrangian (3) unchanged, while the potential becomes

$$U(\sigma + \phi, \boldsymbol{\pi}, \alpha + \alpha_0) = \frac{i}{2}(\alpha_0 + \alpha)(\sigma^2 + \boldsymbol{\pi}^2 + 2\sigma\phi + \phi^2 - v_0^2) + \frac{N\varepsilon}{8}(\alpha_0 + \alpha)^2 - h(\phi + \sigma), \quad (9)$$

In order to derive the Lagrangian from which we can read off the tree-level potential, the tree-level propagators, and the interaction vertices, we use the fact that linear terms in the fields vanish on account of the famous tadpole cancellation which utilizes the definition of the vacuum expectation values via the conditions

$$\frac{dU}{d\phi} \equiv 0, \quad \frac{dU}{d\alpha_0} \equiv 0. \quad (10)$$

The resulting expression for the Lagrangian reads

$$\begin{aligned} \mathcal{L}_{\sigma-\alpha} &= \frac{1}{2}(\partial_\mu\sigma)^2 + \frac{1}{2}(\partial_\mu\boldsymbol{\pi})^2 - \frac{i\alpha_0}{2}\sigma^2 - \frac{i\alpha_0}{2}\boldsymbol{\pi}^2 - \frac{1}{2}\frac{N\varepsilon}{4}\alpha^2 - i\phi\sigma\alpha \\ &\quad - \frac{i}{2}\alpha(\sigma^2 + \boldsymbol{\pi}^2) - U(\phi, \alpha_0), \end{aligned} \quad (11)$$

where the tree-level potential is

$$U(\phi, \alpha_0) = \frac{i}{2}\alpha_0(\phi^2 - v_0^2) + \frac{N\varepsilon}{8}\alpha_0^2 - h\phi. \quad (12)$$

There is a bilinear mixing term, $i\phi\sigma\alpha$, which renders the mass matrix non-diagonal in the fields σ and α .

We can think of two ways to treat this mixing term:

- (i) we keep this term and allow for a non-diagonal propagator which mutually transforms the fields σ and α into each other.
- (ii) we perform a shift,

$$\alpha \longrightarrow \alpha - 4\frac{i\phi}{N\varepsilon}\sigma, \quad (13)$$

which eliminates the bilinear term.

In the following, we discuss the construction of the CJT effective potential only for case (ii). The discussion of case (i) will be delegated to Appendix A where we explicitly demonstrate that, to two-loop order, the effective potential and the equations for the condensates and the masses are the same as for case (ii) when quantities involving the auxiliary field are replaced by their stationary values.

After the shift (13), the resulting expression for the Lagrangian reads

$$\begin{aligned} \bar{\mathcal{L}}_{\sigma-\alpha} &= \frac{1}{2}(\partial_\mu\sigma)^2 + \frac{1}{2}(\partial_\mu\boldsymbol{\pi})^2 - \frac{1}{2}\left(i\alpha_0 + \frac{4\phi^2}{N\varepsilon}\right)\sigma^2 - \frac{1}{2}(i\alpha_0)\boldsymbol{\pi}^2 - \frac{1}{2}\frac{N\varepsilon}{4}\alpha^2 \\ &\quad - \frac{i}{2}\alpha(\sigma^2 + \boldsymbol{\pi}^2) - \frac{2\phi}{N\varepsilon}\sigma(\sigma^2 + \boldsymbol{\pi}^2) - U(\phi, \alpha_0). \end{aligned} \quad (14)$$

From this expression, we can immediately read off the inverse tree-level propagator matrix,

$$\bar{D}^{-1}(K; \phi, \alpha_0) = \begin{pmatrix} \bar{D}_\alpha^{-1} & 0 & 0 & \cdots \\ 0 & \bar{D}_\sigma^{-1}(K; \phi, \alpha_0) & 0 & \cdots \\ 0 & 0 & \bar{D}_\pi^{-1}(K; \alpha_0) & \cdots \\ \vdots & \vdots & & \ddots \end{pmatrix} = \begin{pmatrix} \frac{N\varepsilon}{4} & 0 & 0 & \cdots \\ 0 & -K^2 + i\alpha_0 + \frac{4\phi^2}{N\varepsilon} & 0 & \cdots \\ 0 & 0 & -K^2 + i\alpha_0 & \cdots \\ \vdots & \vdots & & \ddots \end{pmatrix}. \quad (15)$$

The shift (13) has the following consequences:

- (a) the Jacobian associated with the transformation is unity, thus the functional integration in Eq. (7) remains unaffected.
- (b) it generates a term in the σ mass, which diverges in the limit $\varepsilon \rightarrow 0^+$, see Eq. (15). This is expected, since the σ particle becomes infinitely heavy in the nonlinear version of the $O(N)$ model.

Finally, we identify the tree-level vertices from the Lagrangian (11): there are two three-point vertices connecting the auxiliary field α to either two σ or two π fields, respectively. (These are the same vertices that also appear in case (i), see Appendix A.) Furthermore, there is a three-point vertex with three σ fields, and one with one σ and two π -fields. These vertices are proportional to ϕ . (These vertices arise from the shift (13); they do not appear in case (i), see Appendix A.)

B. CJT effective potential

The effective potential assumes the form

$$V_{\text{eff}}(\phi, \alpha_0, G) = U(\phi, \alpha_0) + \frac{1}{2} \int_K [\ln G_\alpha^{-1}(K) + \ln G_\sigma^{-1}(K) + (N-1) \ln G_\pi^{-1}(K)] \\ + \frac{1}{2} \int_K [\bar{D}_\alpha^{-1} G_\alpha(K) + \bar{D}_\sigma^{-1}(K; \phi, \alpha_0) G_\sigma(K) + (N-1) \bar{D}_\pi^{-1}(K; \alpha_0) G_\pi(K) - (N+1)] + V_2(\phi, G), \quad (16)$$

The term $V_2(\phi, G)$ represents the sum of all two-particle irreducible diagrams constructed from the three-point vertices in Eq. (14). By definition, these diagrams consist of at least two loops. The one- and two-point functions are determined by the stationary conditions for the effective potential

$$\frac{\delta V_{\text{eff}}}{\delta \phi} = 0, \quad \frac{\delta V_{\text{eff}}}{\delta \alpha_0} = 0, \quad \frac{\delta V_{\text{eff}}}{\delta G_i(K)} = 0, \quad i = \alpha, \sigma, \pi_1, \dots, \pi_{N-1}. \quad (17)$$

This leads to the following equations for the condensates,

$$h = i\alpha_0\phi + \frac{4\phi}{N\varepsilon} \int_K G_\sigma(K) + \frac{\delta V_2(\phi, G)}{\delta \phi}, \quad (18)$$

$$i\alpha_0 = \frac{2}{N\varepsilon} \left[\phi^2 - v_0^2 + \int_K G_\sigma(K) + (N-1) \int_K G_\pi(K) \right]. \quad (19)$$

For the two-point functions we obtain from Eq. (17) the Dyson equations

$$G_\alpha^{-1}(K) = \bar{D}_\alpha^{-1} + \Pi_\alpha(K), \quad G_\sigma^{-1}(K) = \bar{D}_\sigma^{-1}(K; \phi, \alpha_0) + \Pi_\sigma(K), \quad G_\pi^{-1}(K) = \bar{D}_\pi^{-1}(K; \alpha_0) + \Pi_\pi(K), \quad (20)$$

where the self-energies are

$$\Pi_i(K) = 2 \frac{\delta V_2(\phi, G)}{\delta G_i(K)}, \quad i = \alpha, \sigma, \pi_1, \dots, \pi_{N-1}. \quad (21)$$

In the following two subsections, we give the explicit expressions for the condensate and mass equations in one- and two-loop approximation, respectively.

C. One-loop approximation

In one-loop approximation, $V_2 \equiv 0$. Equation (19) remains the same while Eq. (18) simplifies to

$$h = i\alpha_0\phi + \frac{4\phi}{N\varepsilon} \int_K G_\sigma(K) = \frac{2\phi}{N\varepsilon} \left[\phi^2 - v_0^2 + 3 \int_K G_\sigma(K) + (N-1) \int_K G_\pi(K) \right], \quad (22)$$

where for the second equality we have used Eq. (19) to replace $i\alpha_0$. For $V_2 = 0$, all self-energies are zero, cf. Eq. (21), i.e., the full inverse two-point functions are identical to the inverse tree-level propagators. From Eq. (20) one immediately sees that the two-point functions for σ meson and pion can be written in the form

$$G_i(K) = [\bar{D}_i^{-1}(K; \phi, \alpha)]^{-1} = (-K^2 + M_i^2)^{-1}, \quad i = \sigma, \pi, \quad (23)$$

with the (squared) masses

$$M_\sigma^2 = i\alpha_0 + \frac{4\phi^2}{N\varepsilon} \equiv \frac{2}{N\varepsilon} \left[3\phi^2 - v_0^2 + \int_K G_\sigma(K) + (N-1) \int_K G_\pi(K) \right], \quad (24)$$

$$M_\pi^2 = i\alpha_0 \equiv \frac{2}{N\varepsilon} \left[\phi^2 - v_0^2 + \int_K G_\sigma(K) + (N-1) \int_K G_\pi(K) \right]. \quad (25)$$

For the second equalities we have used the condensate equation (19) to replace $i\alpha_0$. Note that this introduces self-consistently computed tadpole integrals into the equations for the masses.

Neglecting terms which are subleading in $1/N$ — an approximation commonly referred to as the large- N (or Hartree) limit — Eqs. (22), (24), and (25) reduce to

$$h = \phi M_\pi^2 + \mathcal{O}(N^{-1}), \quad (26)$$

$$M_\sigma^2 = M_\pi^2 + \frac{4\phi^2}{N\varepsilon}, \quad (27)$$

$$M_\pi^2 = \frac{2}{N\varepsilon} \left[\phi^2 - v_0^2 + N \int_k G_\pi(k) \right] + \mathcal{O}(N^{-1}). \quad (28)$$

Note that the condensate and the v.e.v. are $\sim \sqrt{N}$, i.e., $\phi^2 \sim v_0^2 \sim N$.

D. Two-loop approximation

To two-loop order there are the four sunset-type diagrams shown in Fig. 1, constructed from the three-point vertices between three σ fields, one σ and two π fields, as well as between one α field with either two σ or two π fields, respectively. There are no double-bubble-type diagrams, due to the absence of four-point vertices. In two-loop approximation,

$$\begin{aligned} V_2(\phi, G) &= \frac{1}{4} \int_K \int_P G_\alpha(K+P) [G_\sigma(K)G_\sigma(P) + (N-1)G_\pi(K)G_\pi(P)] \\ &\quad - \left(\frac{2\phi}{N\varepsilon} \right)^2 \int_K \int_P G_\sigma(K+P) [3G_\sigma(K)G_\sigma(P) + (N-1)G_\pi(K)G_\pi(P)]. \end{aligned} \quad (29)$$

The overall sign follows from the fact that the effective potential has the same sign as the free energy. The combinatorial factors in front of the individual terms follow as usual from counting the possibilities of connecting lines between the vertices, with an overall factor of $1/2$ because there are two vertices.

The condensate equation (19) for the auxiliary field again remains unchanged while Eq. (18) becomes

$$\begin{aligned} h &= i\alpha_0\phi + \frac{4\phi}{N\varepsilon} \int_K G_\sigma(K) - 2\phi \left(\frac{2}{N\varepsilon} \right)^2 \int_K \int_P G_\sigma(K+P) [3G_\sigma(K)G_\sigma(P) + (N-1)G_\pi(K)G_\pi(P)] \\ &= \frac{2\phi}{N\varepsilon} \left\{ \phi^2 - v_0^2 + 3 \int_K G_\sigma(K) + (N-1) \int_K G_\pi(K) \right. \\ &\quad \left. - \frac{4}{N\varepsilon} \int_K \int_P G_\sigma(K+P) [3G_\sigma(K)G_\sigma(P) + (N-1)G_\pi(K)G_\pi(P)] \right\}, \end{aligned} \quad (30)$$

where in the second equality we have used Eq. (19) to replace $i\alpha_0$. This is identical with the condensate equation in the two-loop approximation for the usual $O(N)$ linear σ model without auxiliary field, see Sec. III E.

From Eq. (21) we derive the self-energies as

$$\Pi_\alpha = \frac{1}{2} \int_P [G_\sigma(P)G_\sigma(K-P) + (N-1)G_\pi(P)G_\pi(K-P)], \quad (31)$$

$$\Pi_\sigma(K) = \int_P G_\sigma(P)G_\sigma(K-P) - 2 \left(\frac{2\phi}{N\varepsilon} \right)^2 \int_P [9G_\sigma(P)G_\sigma(K-P) + (N-1)G_\pi(P)G_\pi(K-P)], \quad (32)$$

$$\Pi_\pi(K) = \int_P G_\pi(P)G_\pi(K-P) - 4 \left(\frac{2\phi}{N\varepsilon} \right)^2 \int_P G_\sigma(P)G_\pi(K-P). \quad (33)$$

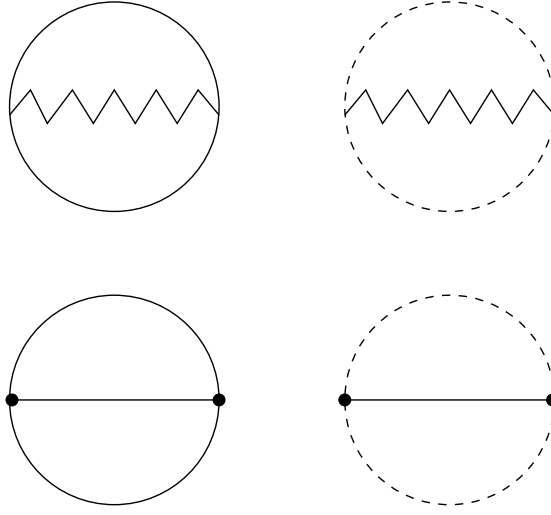


FIG. 1: Two-particle irreducible diagrams constructed from the three-point vertices in Eq. (14). The full line represents the σ field, the dashed line represents the π field and the zigzag line represents the α field.

Then, the Dyson equations (20) for the full two-point functions read

$$G_\alpha^{-1}(K) = \bar{D}_\alpha^{-1} + \Pi_\alpha(K) = \frac{N\varepsilon}{4} + \frac{1}{2} \int_P [G_\sigma(P)G_\sigma(K-P) + (N-1)G_\pi(P)G_\pi(K-P)] , \quad (34)$$

$$\begin{aligned} G_\sigma^{-1}(K) &= \bar{D}_\sigma^{-1}(K; \phi, \alpha_0) + \Pi_\sigma(K) = -K^2 + i\alpha_0 + \frac{4\phi^2}{N\varepsilon} + \Pi_\sigma(K) \\ &= -K^2 + \frac{2}{N\varepsilon} \left[3\phi^2 - v_0^2 + \int_K G_\sigma(K) + (N-1) \int_K G_\pi(K) \right] + \int_P G_\sigma(P)G_\alpha(K-P) \\ &\quad - 2 \left(\frac{2\phi}{N\varepsilon} \right)^2 \int_P [9G_\sigma(P)G_\sigma(K-P) + (N-1)G_\pi(P)G_\pi(K-P)] , \end{aligned} \quad (35)$$

$$\begin{aligned} G_\pi^{-1}(K) &= \bar{D}_\pi^{-1}(K; \alpha_0) + \Pi_\pi(K) = -K^2 + i\alpha_0 + \Pi_\pi(K) \\ &= -K^2 + \frac{2}{N\varepsilon} \left[\phi^2 - v_0^2 + \int_K G_\sigma(K) + (N-1) \int_K G_\pi(K) \right] + \int_P G_\pi(P)G_\alpha(K-P) \\ &\quad - 4 \left(\frac{2\phi}{N\varepsilon} \right)^2 \int_P G_\sigma(P)G_\pi(K-P) . \end{aligned} \quad (36)$$

Here, we have also made use of Eq. (19) for the auxiliary field.

E. Recovering the standard two-loop approximation

In this subsection, we demonstrate that, to two-loop order, the results are the same as for a direct application of the CJT formalism to the original Lagrangian (5) of the $O(N)$ linear σ model (a case that we term “standard two-loop approximation”), if we eliminate the α field using the stationary values for the condensate α_0 and the full propagator G_α . The effective potential for the original $O(N)$ linear σ model reads

$$V_{\text{eff}}^{\text{1}\sigma\text{m}}(\phi, G) = \frac{1}{2N\varepsilon}(\phi^2 - v_0^2)^2 - h\phi + \frac{1}{2} \sum_{i=\sigma,\pi} \int_K [\ln G_i^{-1}(K) + D_i^{-1}(K; \phi)G_i(K) - 1] + V_2^{\text{1}\sigma\text{m}}(\phi, G) , \quad (37)$$

where the inverse tree-level propagators are

$$D_\sigma^{-1}(K; \phi) = -K^2 + \frac{2}{N\varepsilon}(3\phi^2 - v_0^2) , \quad D_\pi^{-1}(K; \phi) = -K^2 + \frac{2}{N\varepsilon}(\phi^2 - v_0^2) , \quad (38)$$

and, to two-loop order,

$$V_2^{1\sigma m}(\phi, G) = \frac{3}{2N\varepsilon} \left[\int_K G_\sigma(K) \right]^2 + (N+1) \frac{N-1}{2N\varepsilon} \left[\int_K G_\pi(K) \right]^2 + \frac{N-1}{N\varepsilon} \int_K G_\pi(K) \int_P G_\sigma(P) \\ - \left(\frac{2\phi}{N\varepsilon} \right)^2 \int_K \int_P G_\sigma(K+P) [3G_\sigma(K)G_\sigma(P) + (N-1)G_\pi(K)G_\pi(P)] . \quad (39)$$

The first line is the contribution from double-bubble diagrams arising from the four-point vertices with four σ fields or two σ and two π fields in the Lagrangian (5). The second line corresponds to the sunset diagrams shown in the second row of Fig. 1. These are the same in the linear σ model with or without auxiliary field. Note that the sunset contribution differs in sign from the double-bubble contribution [this sign was missed in Ref. [25]]. The equation arising from the stationarity condition (17) for $V_{\text{eff}}^{1\sigma m}$ reads

$$h = \frac{2\phi}{N\varepsilon} \left\{ \phi^2 - v_0^2 + 3 \int_K G_\sigma(K) + (N-1) \int_K G_\pi(K) \right. \\ \left. - \frac{4}{N\varepsilon} \int_K \int_P G_\sigma(K+P) [3G_\sigma(K)G_\sigma(P) + (N-1)G_\pi(K)G_\pi(P)] \right\} . \quad (40)$$

This is identical with Eq. (30), i.e., with the equation obtained via the auxiliary-field formalism, once the auxiliary field is eliminated with the help of Eq. (19).

The self-energies for σ meson and pion read

$$\Pi_\sigma^{1\sigma m}(K) = \frac{2}{N\varepsilon} \left[3 \int_K G_\sigma(K) + (N-1) \int_K G_\pi(K) \right] \\ - 2 \left(\frac{2\phi}{N\varepsilon} \right)^2 \int_P [9G_\sigma(P)G_\sigma(K-P) + (N-1)G_\pi(P)G_\pi(K-P)] , \quad (41)$$

$$\Pi_\pi^{1\sigma m}(K) = \frac{2}{N\varepsilon} \left[\int_K G_\sigma(K) + (N+1) \int_K G_\pi(K) \right] - 4 \left(\frac{2\phi}{N\varepsilon} \right)^2 \int_P G_\pi(P)G_\sigma(K-P) . \quad (42)$$

Therefore, the Dyson equations for the full two-point functions read

$$G_\sigma^{-1}(K) = D_\sigma^{-1}(K; \phi) + \Pi_\sigma^{1\sigma m}(K) \\ = -K^2 + \frac{2}{N\varepsilon}(3\phi^2 - v_0^2) + \frac{2}{N\varepsilon} \left[3 \int_K G_\sigma(K) + (N-1) \int_K G_\pi(K) \right] \\ - 2 \left(\frac{2\phi}{N\varepsilon} \right)^2 \int_P [9G_\sigma(P)G_\sigma(K-P) + (N-1)G_\pi(P)G_\pi(K-P)] , \quad (43)$$

$$G_\pi^{-1}(K) = D_\pi^{-1}(K; \phi) + \Pi_\pi^{1\sigma m}(K) \\ = -K^2 + \frac{2}{N\varepsilon}(\phi^2 - v_0^2) + \frac{2}{N\varepsilon} \left[\int_K G_\sigma(K) + (N+1) \int_K G_\pi(K) \right] - 4 \left(\frac{2\phi}{N\varepsilon} \right)^2 \int_P G_\pi(P)G_\sigma(K-P) . \quad (44)$$

These equations are identical with the Dyson equations (35) and (36), if we replace the propagator G_α of the auxiliary field in those equations using the Dyson equation (34). In order to see this, we formally write

$$G_\alpha(K) = [G_\alpha^{-1}(K)]^{-1} = [\bar{D}_\alpha^{-1} + \Pi_\alpha(K)]^{-1} = \bar{D}_\alpha \sum_{n=0}^{\infty} [-\bar{D}_\alpha \Pi_\alpha(K)]^n . \quad (45)$$

If we insert this into the respective terms in Eqs. (35) and (36), we observe that the terms for $n \geq 1$ generate contributions which are at least of second order in loops (because $\Pi_\alpha(K)$ is already a one-loop term). However, to two-loop order in the effective potential, it is sufficient to consider the 1PI self-energies to one-loop order only. Therefore, we may neglect all contributions in Eq. (45) except for the $n=0$ (tree-level) term. Then, we may replace

$$\int_P G_i(P)G_\alpha(K-P) \longrightarrow \int_P G_i(P)\bar{D}_\alpha = \frac{4}{N\varepsilon} \int_P G_i(P) , \quad i = \sigma, \pi , \quad (46)$$

in Eqs. (35) and (36), i.e., they become simple tadpole contributions to the self-energies. Combining these with the other tadpole contributions, we observe that, indeed, Eqs. (35) and (36) become identical with Eqs. (43) and (44).

Finally, we also show that the effective potential (29) in two-loop approximation for $V_2(\phi, G)$, Eq. (29), becomes identical with the effective potential for the standard linear σ model, Eq. (39), if we replace the expectation value and the full two-point function for the auxiliary field by their stationary values. To this end, it is advantageous to consider the tree-level, the one-loop, and the two-loop contributions in Eq. (16) separately. The tree-level potential at the stationary value for α_0 reads

$$\begin{aligned} U(\phi, \alpha_0) &= \frac{1}{2}(\phi^2 - v_0^2) \frac{2}{N\varepsilon} \left[\phi^2 - v_0^2 + \int_K G_\sigma(K) + (N-1) \int_K G_\pi(K) \right] \\ &\quad - \frac{N\varepsilon}{8} \left(\frac{2}{N\varepsilon} \right)^2 \left[\phi^2 - v_0^2 + \int_K G_\sigma(K) + (N-1) \int_K G_\pi(K) \right]^2 - h\phi \\ &= \frac{1}{2N\varepsilon} \left\{ \phi^2 - v_0^2 - \left[\int_K G_\sigma(K) \right]^2 - 2(N-1) \int_K G_\sigma(K) \int_P G_\pi(P) - (N-1)^2 \left[\int_K G_\pi(K) \right]^2 \right\} - h\phi. \end{aligned} \quad (47)$$

For the one-loop contribution, we expand the logarithm of the inverse two-point function for the auxiliary field using the Dyson equation (34) and employ the expansion (45),

$$\begin{aligned} \ln G_\alpha^{-1}(K) + \bar{D}_\alpha^{-1} G_\alpha(K) - 1 &= \ln \bar{D}_\alpha^{-1} + \ln [1 + \bar{D}_\alpha \Pi_\alpha(K)] + \bar{D}_\alpha^{-1} [\bar{D}_\alpha^{-1} + \Pi_\alpha(K)]^{-1} - 1 \\ &= \ln \frac{N\varepsilon}{4} + \bar{D}_\alpha \Pi_\alpha(K) - \sum_{n=2}^{\infty} \frac{1}{n} [-\bar{D}_\alpha \Pi_\alpha(K)]^n + 1 - \bar{D}_\alpha \Pi_\alpha(K) + \sum_{n=2}^{\infty} [-\bar{D}_\alpha \Pi_\alpha(K)]^n - 1 \\ &= \ln \frac{N\varepsilon}{4} + \sum_{n=2}^{\infty} [-\bar{D}_\alpha \Pi_\alpha(K)]^n \left(1 - \frac{1}{n} \right). \end{aligned} \quad (48)$$

We observe that the terms linear in $\Pi_\alpha(K)$ as well as the unit terms cancel. In the final result, the first term is a (negligible) constant. The remaining series starts with a term with two powers of $\Pi_\alpha(K)$. Since $\Pi_\alpha(K)$ is (at least) of one-loop order, when integrating over K , this term is (at least) of three-loop order in the effective potential. (In fact, since $\bar{D}_\alpha = 4/(N\varepsilon) = \text{const.}$, one readily convinces oneself that the $n = 2$ term in the series corresponds to the well-known basketball diagram.) To two-loop order in the effective potential, we may therefore neglect the series in Eq. (48).

Using Eq. (19), the remaining one-loop terms in the effective potential (16) read

$$\begin{aligned} &\frac{1}{2} \int_K [\ln G_\sigma^{-1}(K) + (N-1) \ln G_\pi^{-1}(K) + \bar{D}_\sigma^{-1}(K; \phi, \alpha_0) G_\sigma(K) + (N-1) \bar{D}_\pi^{-1}(K; \alpha_0) G_\pi(K) - N] \\ &= \frac{1}{2} \int_K \left\{ \ln G_\sigma^{-1}(K) + (N-1) \ln G_\pi^{-1}(K) \right. \\ &\quad \left. + \left[-K^2 + \frac{2}{N\varepsilon} (3\phi^2 - v_0^2) \right] G_\sigma(K) + (N-1) \left[-K^2 + \frac{2}{N\varepsilon} (\phi^2 - v_0^2) \right] G_\pi(K) - N \right\} \\ &\quad + \frac{1}{N\varepsilon} \left[\int_K G_\sigma(K) + (N-1) \int_K G_\pi(K) \right]^2, \end{aligned} \quad (49)$$

where the last term arises from the tadpole contributions to Eq. (19). Multiplying them with full two-point functions $G_\sigma(K)$, $G_\pi(K)$, and integrating over K , they lead to the double-bubble-type terms shown in the last line. Note that the coefficients of the full two-point functions in the second line are just the inverse tree-level propagators in the standard linear σ model, cf. Eq. (38).

Finally, we consider the two-loop contribution (29). To two-loop order, it is justified to replace $G_\alpha(K+P) \rightarrow \bar{D}_\alpha \equiv 4/(N\varepsilon)$, and we obtain

$$\begin{aligned} V_2(\phi, G) &\simeq \frac{1}{N\varepsilon} \left\{ \left[\int_K G_\sigma(K) \right]^2 + (N-1) \left[\int_K G_\pi(K) \right]^2 \right\} \\ &\quad - \left(\frac{2\phi}{N\varepsilon} \right)^2 \int_K \int_P G_\sigma(K+P) [3G_\sigma(K)G_\sigma(P) + (N-1)G_\pi(K)G_\pi(P)]. \end{aligned} \quad (50)$$

Adding Eqs. (47), (48), and (49), we indeed obtain the effective potential (39) of the standard linear σ model.

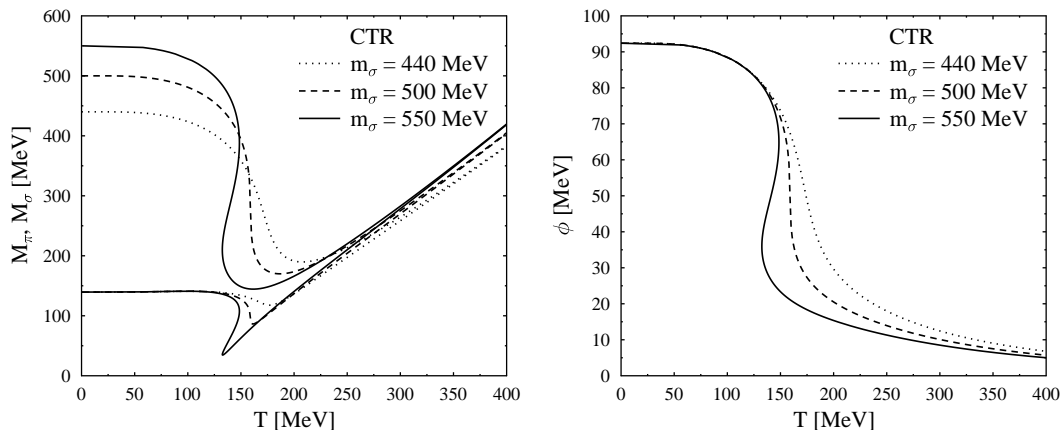


FIG. 2: The pion mass, the sigma mass, and the condensate as a function of T in the $O(4)$ linear σ model in case of explicitly broken symmetry using the CTR scheme for different values of m_σ .

IV. RESULTS

In this section, we show numerical solutions for the one-loop approximation, Eqs. (22), (24), and (25), for $N = 4$, corresponding to a system of three pions and their chiral partner, the σ particle. We compare this to results for the one-loop approximation in the large- N limit, Eqs. (26) – (28). We discuss the results for the linear and the nonlinear σ model, with and without explicitly broken chiral symmetry. Furthermore, we investigate the counterterm renormalisation (CTR) method discussed in Appendix B and the so-called trivial regularization (TR) where the vacuum contribution of the tadpole integral is set to zero. This is strictly speaking not an entirely consistent procedure because these “vacuum” contributions actually have an implicit temperature dependence: they depend on the self-consistently computed particle masses which are functions of temperature. On the other hand, the CTR method does not have this shortcoming because the counter terms used to eliminate the divergences are (infinite) constants independent of temperature.

In the TR method the parameters are determined by solving Eqs. (22), (24), and (25) in the vacuum,

$$h = m_\pi^2 f_\pi, \quad \frac{1}{\varepsilon} = \frac{m_\sigma^2 - m_\pi^2}{f_\pi^2}, \quad v_0^2 = f_\pi^2 - 2\varepsilon m_\pi^2. \quad (51)$$

Similarly, in the CTR method the parameters are obtained from the solutions of the renormalized equations (B16), (B17), and (B18) at $T = 0$,

$$h = f_\pi \left[m_\pi^2 + \frac{1}{16\pi^2\varepsilon} \left(m_\sigma^2 \ln \frac{m_\sigma^2}{\mu^2} - m_\sigma^2 + \mu^2 \right) \right], \quad \frac{1}{\varepsilon} = \frac{m_\sigma^2 - m_\pi^2}{f_\pi^2},$$

$$v_0^2 = f_\pi^2 - 2\varepsilon m_\pi^2 + \frac{1}{16\pi^2} \left[m_\sigma^2 \ln \frac{m_\sigma^2}{\mu^2} - m_\sigma^2 + \mu^2 + 3 \left(m_\pi^2 \ln \frac{m_\pi^2}{\mu^2} - m_\pi^2 + \mu^2 \right) \right]. \quad (52)$$

Note that, in the chiral limit, $h \rightarrow 0^+$, where $m_\pi \rightarrow 0$, the first equation requires to choose the renormalization scale $\mu = m_\sigma$.

A. Linear model with explicitly broken symmetry

In Fig. 2 we show the masses of the pion and the σ meson, as well as the condensate as a function of temperature for different values of the vacuum σ mass m_σ . One observes that the condensate decreases as a function of temperature, which is a consequence of the restoration of chiral symmetry. Depending on the value of m_σ , chiral symmetry restoration may proceed via a phase transition. In the CTR scheme, the phase transition is of second order for $m_\sigma \simeq 500$ MeV, and of first order for larger values of m_σ . For smaller values, however, the transition is only crossover. In the chirally restored phase, the condensate is always nonzero because of the small explicit breaking

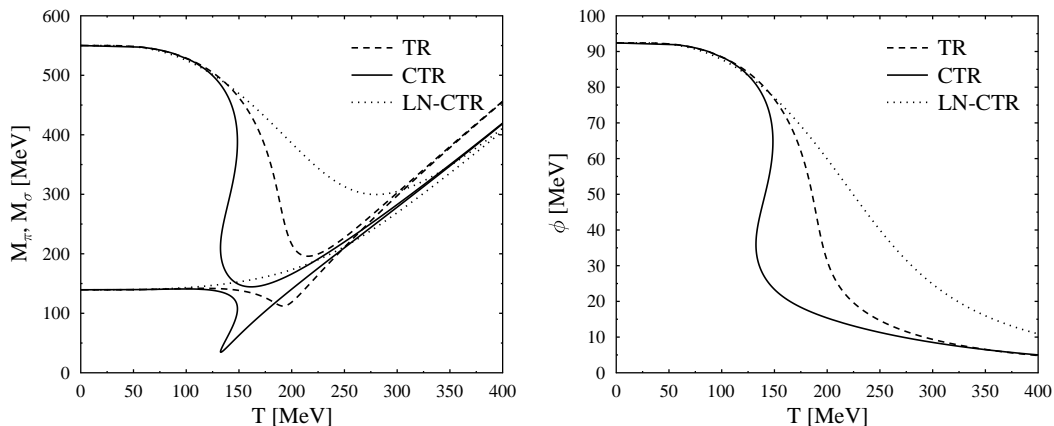


FIG. 3: The pion mass, the sigma mass, and the condensate as a function of T in the $O(4)$ linear model in case of explicitly broken symmetry for $m_\sigma = 550$ MeV and different renormalization schemes.

of chiral symmetry due to non-vanishing quark masses (which gives rise to a nonzero pion mass $m_\pi = 139.5$ MeV). Since the results for the TR method are qualitatively similar, we do not show them explicitly, but we remark that the second-order transition occurs for larger values of the vacuum σ mass, $m_\sigma \simeq 700$ MeV. Note that a crossover transition is also found in lattice QCD calculations [3]. This, however, does not imply that the mass of the σ meson as the chiral partner of the pion must be small. In fact, the identification of the chiral partner of the pion is a long-debated issue, see Refs. [36] and refs. therein.

Figure 3 shows the effect of different regularization resp. renormalization schemes, as well as different approximation schemes on the behavior of the masses and the condensate as functions of temperature. We keep the vacuum mass of the σ meson fixed to $m_\sigma = 550$ MeV. In the CTR scheme, the system exhibits a first-order phase transition. When using the TR method, however, one observes a crossover transition. In the large- N limit with CTR, the chiral transition is always crossover, independent of the mass of the σ meson. In Fig. 3, the crossover transition is observed to be smoother for the large- N approximation with CTR than for the other cases. In fact, with this renormalization scheme, the smoothness is proportional to m_σ . We shall see in the next section that the transition disappears as we approach the nonlinear limit $m_\sigma \rightarrow \infty$. This, however, does not happen for the TR method.

B. Nonlinear model with explicitly broken symmetry

In the nonlinear model the results are obtained by solving (the properly renormalized) Eqs. (22), (24), and (25) in the limit $\varepsilon \rightarrow 0^+$. Because of the relation $1/\varepsilon = (m_\sigma^2 - m_\pi^2)/f_\pi^2$, Eqs. (51) and (52), the nonlinear limit is equivalent to sending m_σ to infinity. In this case, when the TR method is used, the phase transition is of first order, with a rather large discontinuity in the condensate at a critical temperature of $T_c \simeq 178.6$ MeV, see Fig. 4. The condensate is very small above T_c , but still nonzero, because of explicit symmetry breaking. The first-order nature of the transition is in line with the expectation from the linear case, where the transition becomes first order when the σ mass is sufficiently large. Below T_c the σ mass is infinitely heavy and there are only pionic excitations. Above T_c the masses of σ meson and pion become degenerate.

In the large- N limit of the one-loop approximation and with the TR method, the phase transition is crossover with $T_c \simeq 185$ MeV, see Fig. 5. In this case the σ field remains infinitely heavy also above T_c . This is the main difference to the previous case, where the σ meson becomes degenerate with the pion above T_c . It is at first sight surprising that this small difference can cause such a drastic change in the order of the phase transition. The explanation lies in a comparison of the equations in the one-loop approximation (22), (24), and (25) with those in the large- N limit, Eqs. (26) – (28). Since the σ meson is infinitely heavy below T_c , there is no contribution from this mode to these equations. However, above T_c , thermal fluctuations of the σ meson can contribute in the one-loop approximation, while they remain absent in the large- N limit of the one-loop approximation. This is sufficient to drive the transition to first order in the one-loop approximation.

In the one-loop approximation and using the CTR scheme, the parameter space of the model does not give physically meaningful solutions in the nonlinear case $m_\sigma \rightarrow \infty$. In this case, $\phi \rightarrow 0$ and $M_\sigma, M_\pi \rightarrow \infty$ for all values of T . On the

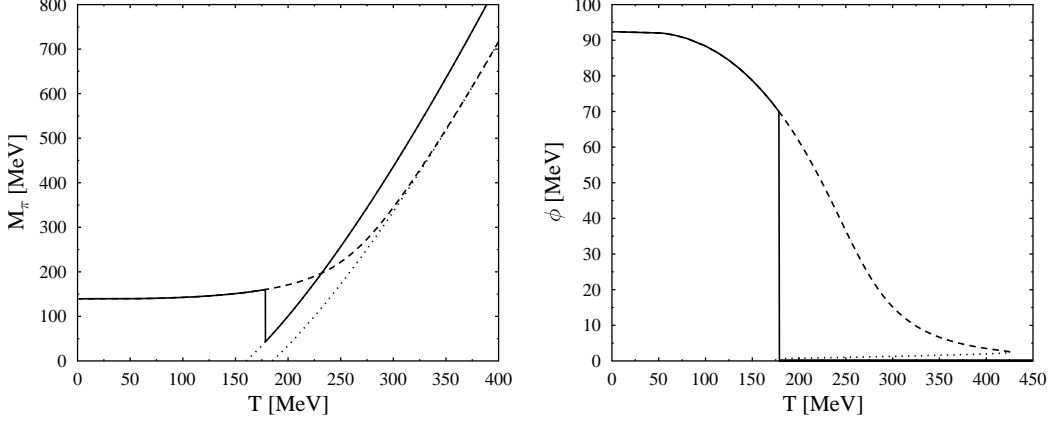


FIG. 4: The pion mass and the condensate as a function of T in the $O(4)$ nonlinear model in case of explicitly broken symmetry using the TR-scheme for $m_\sigma \rightarrow \infty$ (in practice $m_\sigma = 250$ GeV is used). The solid line shows the physical case which corresponds to the global minimum of the effective potential. The dashed and dotted lines show the unstable or metastable solution of the gap equations, which corresponds to the local minimum (dashed) or maximum (dotted) of the effective potential.

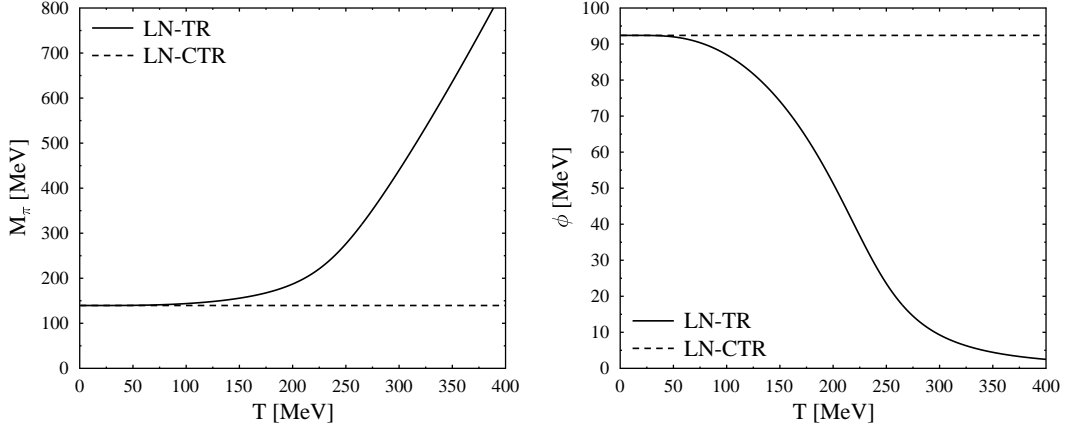


FIG. 5: The pion mass and the condensate as a function of T in the $O(4)$ nonlinear model in case of explicitly broken symmetry using the large- N approximation in the TR-scheme (full) and CTR-scheme (dashed) for $m_\sigma \rightarrow \infty$.

other hand, the large- N limit of the one-loop approximation allows for a solution, however, the transition disappears completely, the condensate and the masses retain their constant tree-level values for all $T > 0$: $\phi = f_\pi$, $M_\sigma = m_\sigma$, $M_\pi = m_\pi$, see Fig. 5.

C. Linear model in the chiral limit

The chiral limit is obtained by taking $h \rightarrow 0^+$. Combining Eqs. (22) and (25) we see that

$$\phi \left[M_\pi^2 + \frac{4}{N\varepsilon} \int_K G_\sigma(K) \right] = h \longrightarrow 0^+, \quad (53)$$

which can only be fulfilled if the σ tadpole exactly cancels M_π^2 . This, however, is only possible, if the pion becomes tachyonic, $M_\pi^2 < 0$, since the thermal as well as the (finite) vacuum contribution to the tadpole are always positive (semi-)definite. As a consequence, we can only show results in the large- N limit, since there this problem is absent, cf. Eqs. (26).

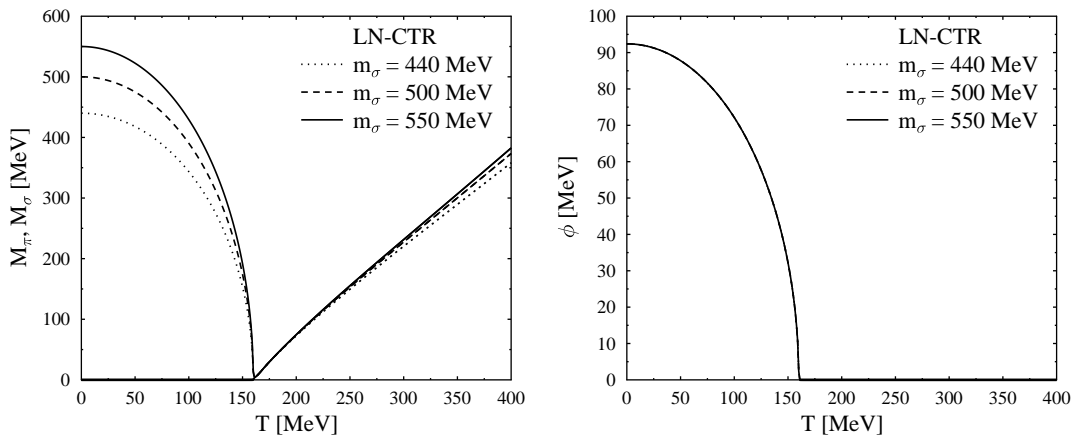


FIG. 6: The pion mass, the sigma mass, and the condensate as a function of T in the large- N limit of the one-loop approximation of the $O(4)$ linear σ model in the chiral limit.

In Fig. 6 we show the behavior of the masses and the condensate as functions of temperature for various values of the vacuum σ mass in the large- N limit in the CTR scheme (the results for the TR method are qualitatively similar, therefore we do not show them explicitly). The results of Fig. 6 are in agreement with universality class arguments which predict a second-order phase transition. In the phase where chiral symmetry is spontaneously broken the pions are massless in accordance with Goldstone's theorem. Above the critical temperature the chiral partners become degenerate in mass. The condensate as a function of temperature is independent of the value of m_σ . This can be seen as follows. We subtract Eq. (28) at $T = 0$ (where $\phi = f_\pi$) from the same equation at an arbitrary temperature $T \leq T_c$, where T_c is the phase transition temperature. Since in the phase of broken chiral symmetry we always have $M_\pi \equiv 0$, the result is

$$0 = \phi^2(T) - f_\pi^2 + N \frac{T^2}{12}, \quad (54)$$

where the thermal contribution to the tadpole integral could be determined analytically at all temperatures $T \leq T_c$ because $M_\pi = 0$. The term v_0^2 , as well as the vacuum contributions to the tadpole integrals cancel when taking the difference. The critical temperature T_c can be easily deduced from Eq. (54) noting that $\phi(T_c) = 0$. The result is $T_c = \sqrt{12/N} f_\pi = \sqrt{3} f_\pi$.

D. Nonlinear model in the chiral limit

In the chiral limit of the nonlinear $O(N)$ model both parameters ε and h must be sent to zero. In the one-loop approximation and in the TR method, pions respect Goldstone's theorem by remaining massless in the phase of spontaneously broken chiral symmetry, see Fig. 7. In this phase, the σ field is effectively frozen out due to its infinite mass. There is a first-order phase transition at a critical temperature $T_c = \sqrt{3} f_\pi$. At this temperature, the condensate drops to zero discontinuously, while the pion mass starts to increase continuously from zero above this temperature. In the restored phase, the σ meson becomes degenerate in mass with the pions. This is the reason why T_c assumes the same value as in the large- N limit of the linear model. When inspecting Eqs. (24) and (25), we observe that they become identical with Eqs. (27) and (28) for $M_\sigma = M_\pi = 0$ in the chiral limit and above T_c (where $\phi = 0$). Therefore, we obtain the same equation (54) that determines the value of T_c as in the linear case in the large- N limit.

However, in the one-loop approximation in the CTR scheme no physical solutions can be obtained: the condensate goes to zero, $\phi \rightarrow 0$, and the masses of σ meson and pion go to infinity, $M_\sigma, M_\pi \rightarrow \infty$. This situation is similar to the nonlinear case with explicit symmetry breaking.

In the large- N limit, the phase transition is of second order with a critical temperature $T_c = \sqrt{3} f_\pi$, both in the TR method and in the CTR scheme, see Fig. 8. Below T_c the σ mass is infinite, while the pions are massless, respecting Goldstone's theorem. Above the critical temperature the masses of the chiral partners become degenerate, $M_\sigma = M_\pi > 0$ in the TR scheme, and $M_\sigma = M_\pi = 0$ in the CTR scheme. At first sight, it is surprising that the σ field becomes massless above T_c . This behavior can be traced to our choice of the renormalization scale $\mu = m_\sigma \rightarrow \infty$.

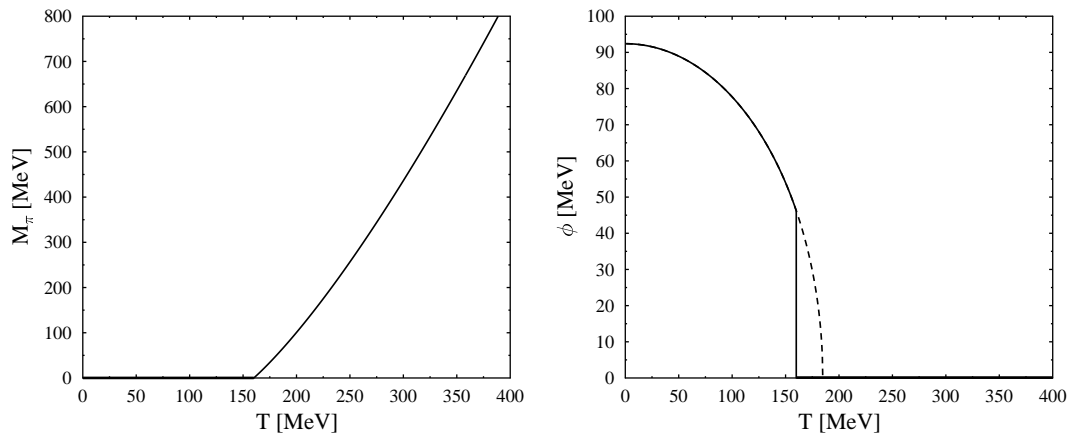


FIG. 7: The pion mass and the condensate as a function of T in the $O(4)$ nonlinear model in the chiral limit using the TR-scheme for $m_\sigma \rightarrow \infty$ (in practice $m_\sigma = 250$ GeV is used). The solid line corresponds to the physical case. The dashed line shows the metastable solution of the gap equations which corresponds to the local minimum of the effective potential.

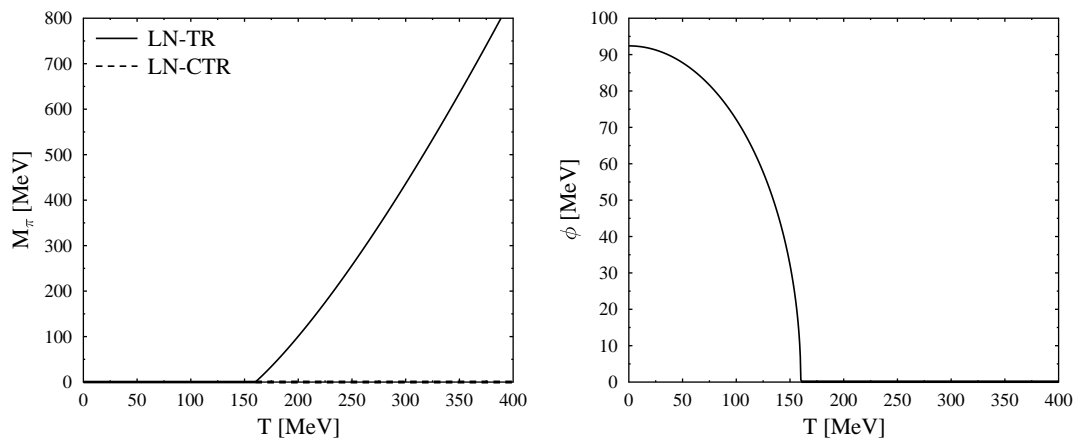


FIG. 8: The pion mass and the condensate as a function of T in the $O(4)$ nonlinear model in the chiral limit using the large- N approximation at one-loop order in the TR-scheme (full) and CTR-scheme (dashed) for $m_\sigma \rightarrow \infty$.

In fact, this is similar to what was observed in Ref. [13] (cf. Fig. 3 of that work), when increasing the renormalization scale in the large- N limit in the CTR scheme.

V. CONCLUSIONS

In this work we have investigated the linear and the nonlinear $O(N)$ model at nonzero temperature. An auxiliary field has been used to derive the effective potential. This method allowed us to establish a simple and mathematically rigorous relation between the linear and nonlinear versions of the model. This also leads to differences when comparing our results with previous treatments of the $O(N)$ model, see below. The equations for the temperature-dependent masses and the condensate were derived using the CJT formalism. We explicitly showed that, up to two-loop order, the auxiliary-field method is equivalent to the standard $O(N)$ linear σ model, once the one- and two-point functions involving the auxiliary field are replaced by their stationary values. In order to regularize the divergent vacuum terms we applied the counter-term (CTR) scheme as well as the so-called trivial regularization (TR) method where divergent terms are simply ignored.

Table I shows a compilation of the results for the various scenarios studied in this paper. The first row summarizes

	CTR	CTR	TR	TR	LN-CTR	LN-CTR	LN-TR	LN-TR
	$m_\pi = m_\pi^{phys}$	$m_\pi \rightarrow 0^+$	$m_\pi = m_\pi^{phys}$	$m_\pi \rightarrow 0^+$	$m_\pi = m_\pi^{phys}$	$m_\pi \rightarrow 0^+$	$m_\pi = m_\pi^{phys}$	$m_\pi \rightarrow 0^+$
lin	second order at $m_\sigma \simeq 500$ MeV	\otimes	second order at $m_\sigma \simeq 750$ MeV	\otimes	crossover	second order $T_c = \sqrt{\frac{12}{N}} f_\pi$	crossover	second order $T_c = \sqrt{\frac{12}{N}} f_\pi$
nonlinear	\otimes	\otimes	first order	first order $T_c = \sqrt{\frac{12}{N}} f_\pi$	no transition	second order $T_c = \sqrt{\frac{12}{N}} f_\pi$	crossover	second order $T_c = \sqrt{\frac{12}{N}} f_\pi$

TABLE I: Summary of cases studied in this paper. The symbol \otimes indicates that no reasonable result can be obtained due to tachyonic pion propagation. In those cases the phase transition becomes cross-over for smaller sigma masses and of first order for sigma masses higher than the shown values. $m_\pi = m_\pi^{phys}$ corresponds to the physical case of nonzero quark masses, $m_\pi^{phys} = 139.5$ MeV.

the results for the linear case, while the second those for the nonlinear case. In the first four columns we show the results for the one-loop approximation, the first two for the CTR scheme and the next two for the TR method, for the case of explicit chiral symmetry breaking and in the chiral limit. The last four columns show the corresponding results for the large- N limit of the one-loop approximation. In the cases indicated with a \otimes , we were not able to find physically acceptable solutions due to tachyonic pion propagation. In all other cases, we indicated the nature of the phase transition and, if independent of the σ mass, the critical temperature. As one observes, $T_c = \sqrt{12/N} f_\pi \equiv \sqrt{3} f_\pi$ in the chiral limit for all scenarios, independent of the details (linear vs. nonlinear, or CTR vs. TR, or one-loop approximation vs. large- N limit). In the cases where the order of the transition depends on the σ mass, we indicated the value of m_σ where the transition is of second order; it is crossover for smaller and of first order for larger values of m_σ .

We now compare our results to previous work. In Ref. [13], the $O(N)$ model for $N = 4$ was studied in the CJT formalism without using the auxiliary-field method. Although not studied in that work, we repeated the respective calculations varying the σ mass. We find that, in the Hartree-Fock approximation (erroneously named ‘‘Hartree approximation’’ in that paper) and in the case of explicitly broken chiral symmetry, the phase transition changes from crossover to first order for $m_\sigma \simeq 940$ MeV in the TR method and for $m_\sigma \simeq 680$ MeV in the CTR scheme. This is consistent with our results obtained with the auxiliary-field method, although the critical values for m_σ are somewhat larger for the method of Ref. [13]. In the chiral limit, the method of Ref. [13] yields a first-order phase transition for all m_σ values. Furthermore, Goldstone’s theorem is not fulfilled due to a non-vanishing pion mass in the phase of broken chiral symmetry. In the large- N limit, the results of Ref. [13] coincide with ours, since the effective potentials are identical.

The auxiliary-field method has been applied previously to examine properties of the $O(N)$ model to leading [28, 29] and next-to-leading order in the $1/N$ expansion [30, 31]. To leading order in $1/N$ the σ and π fields have the same mass irrespective of whether chiral symmetry is explicitly or only spontaneously broken. Thus, in the chiral limit there are four instead of three massless bosons. The phase transition is of second order with a critical temperature of $T_c = \sqrt{12/N} f_\pi$. In the case of explicitly broken symmetry there is a crossover phase transition and four massive particles. The key difference in our study to the afore mentioned Refs. [28, 29] is the correct treatment of the limiting process regarding the constraint imposed by the nonlinearity: the σ mass is therefore infinite in the phase of broken symmetry. To next-to-leading order including renormalization [30] the results change as follows: in the chiral limit there are three Goldstone bosons since the σ field becomes massive. The phase transition is of second (or higher) order. In the weak-coupling limit the critical temperature is $T_c = \sqrt{12/(N+2)} f_\pi$ and above the critical temperature the masses of the chiral partners become degenerate.

A natural next step is the extension to nonzero chemical potentials [31]. A further interesting study would be the inclusion of additional scalar singlet states [37]. Finally, the application of the auxiliary-field method should also be instructive for more complicated systems incorporating additional vector and axial vector mesonic degrees of freedom [38].

Acknowledgement

The authors thank T. Brauner, M. Grahl, A. Heinz, S. Leupold, and H. Warringa for interesting discussions. The work of E. Seel was supported by the Helmholtz Research School ‘‘H-QM’’. We thank the referee for valuable comments which lead to a substantial modification of an earlier version of this manuscript, and in particular to the calculations presented in Sec. III E and Appendix A.

Appendix A: CJT effective potential with non-diagonal propagator

In this appendix, we discuss the CJT effective potential for the case where we do not perform a shift of the α field (denoted as case (i) in Sec. III). Due to the appearance of non-diagonal propagators which mix the α and σ fields, this is more complicated than the case discussed in the main part of the paper.

1. Tree-level propagators, and vertices

The starting point is the Lagrangian (11), with the tree-level potential (12). From this, we immediately deduce the tree-level propagator matrix as

$$D^{-1}(K; \phi, \alpha_0) = \begin{pmatrix} D_{\alpha\alpha}^{-1} & D_{\alpha\sigma}^{-1}(\phi) & 0 & \cdots \\ D_{\sigma\alpha}^{-1}(\phi) & D_{\sigma\sigma}^{-1}(K; \alpha_0) & 0 & \cdots \\ 0 & 0 & D_{\pi\pi}^{-1}(K; \alpha_0) & \\ \vdots & \vdots & & \ddots \end{pmatrix} = \begin{pmatrix} \frac{N\varepsilon}{4} & i\phi & 0 & \cdots \\ i\phi & -K^2 + i\alpha_0 & 0 & \cdots \\ 0 & 0 & -K^2 + i\alpha_0 & \\ \vdots & \vdots & & \ddots \end{pmatrix}. \quad (\text{A1})$$

Note the following relations between the inverse tree-level propagators in the shifted, Eq. (15), and unshifted, Eq. (A1), cases: $\bar{D}_{\alpha}^{-1} \equiv D_{\alpha\alpha}^{-1}$ and $\bar{D}_{\pi}^{-1}(K; \alpha_0) \equiv D_{\pi\pi}^{-1}(K; \alpha_0)$, while $\bar{D}_{\sigma}^{-1}(K; \phi, \alpha_0) = D_{\sigma\sigma}^{-1}(K; \alpha_0) + 4\phi^2/(N\varepsilon)$.

The Lagrangian (11) contains only two three-point tree-level vertices, where one α field interacts with either two σ or two π fields, respectively. These are the same vertices that also appear in case (ii), see Sec. III A.

2. CJT effective potential

The CJT effective potential assumes the form

$$V_{\text{eff}}(\phi, \alpha_0, G) = U(\phi, \alpha_0) + \frac{1}{2} \int_K \text{Tr} [\ln G^{-1}(K) + D^{-1}(K; \phi, \alpha_0) G(K) - 1] + V_2(G), \quad (\text{A2})$$

where the two-point function $G(K)$ is an $(N+1) \times (N+1)$ -matrix, just like the inverse tree-level propagator $D^{-1}(K; \phi, \alpha_0)$ in Eq. (A1). The term $V_2(G)$ represents the sum of all two-particle irreducible diagrams constructed from $G(K)$ and the two different three-point vertices in Eq. (11) (which do not depend on the one-point functions ϕ and α_0).

The stationary conditions for the effective potential are given by

$$\frac{\delta V_{\text{eff}}}{\delta \phi} = 0, \quad \frac{\delta V_{\text{eff}}}{\delta \alpha_0} = 0, \quad \frac{\delta V_{\text{eff}}}{\delta G_{ij}(K)} = 0, \quad i, j = \alpha, \sigma, \pi_1, \dots, \pi_{N-1}. \quad (\text{A3})$$

This leads to the following equations for the two condensates ϕ and α_0

$$h = i\alpha_0\phi + \frac{i}{2} \int_K [G_{\sigma\alpha}(K) + G_{\alpha\sigma}(K)], \quad (\text{A4})$$

$$i\alpha_0 = \frac{2}{N\varepsilon} \left[\phi^2 - v_0^2 + \int_K G_{\sigma\sigma}(K) + (N-1) \int_K G_{\pi\pi}(K) \right]. \quad (\text{A5})$$

The equation for ϕ is now different from case (ii), see Eq. (18), but the equation for α_0 remains the same, cf. Eq. (19). The two-point function has the matrix elements

$$G_{ji}^{-1}(K) = D_{ji}^{-1}(K; \phi, \alpha_0) + \Pi_{ji}(K), \quad (\text{A6})$$

where the one-particle irreducible (1PI) self-energy is

$$\Pi_{ji}(K) = 2 \frac{\delta V_2(G)}{\delta G_{ij}(K)}, \quad i, j = \alpha, \sigma, \pi_1, \dots, \pi_{N-1}. \quad (\text{A7})$$

It is instructive to formally invert the full inverse two-point function G^{-1} in order to obtain the full two-point function G . From the Dyson equation (A6) we observe that G^{-1} has a similar matrix structure as the inverse tree-level propagator (A1). We assume that inverting G^{-1} preserves this structure, i.e.,

$$G = \begin{pmatrix} G_{\alpha\alpha} & G_{\alpha\sigma} & 0 & \cdots \\ G_{\sigma\alpha} & G_{\sigma\sigma} & 0 & \cdots \\ 0 & 0 & G_{\pi\pi} & \\ \vdots & \vdots & & \ddots \end{pmatrix}. \quad (\text{A8})$$

Obviously, $G_{\pi\pi} = (G_{\pi\pi}^{-1})^{-1}$. However, inverting the 2×2 matrix corresponding to the $\alpha - \sigma$ sector is more complicated. From the condition

$$\begin{pmatrix} 1 & 0 \\ 0 & 1 \end{pmatrix} = \begin{pmatrix} G_{\alpha\alpha}^{-1} & G_{\alpha\sigma}^{-1} \\ G_{\sigma\alpha}^{-1} & G_{\sigma\sigma}^{-1} \end{pmatrix} \begin{pmatrix} G_{\alpha\alpha} & G_{\alpha\sigma} \\ G_{\sigma\alpha} & G_{\sigma\sigma} \end{pmatrix} \quad (\text{A9})$$

we obtain

$$\begin{aligned} G_{\alpha\alpha} &= \left[G_{\alpha\alpha}^{-1} - G_{\alpha\sigma}^{-1} \frac{1}{G_{\sigma\sigma}^{-1}} G_{\sigma\alpha}^{-1} \right]^{-1}, \\ G_{\sigma\sigma} &= \left[G_{\sigma\sigma}^{-1} - G_{\sigma\alpha}^{-1} \frac{1}{G_{\alpha\alpha}^{-1}} G_{\alpha\sigma}^{-1} \right]^{-1}, \\ G_{\alpha\sigma} &= -\frac{1}{G_{\alpha\alpha}^{-1}} G_{\alpha\sigma}^{-1} G_{\sigma\sigma} = \left[G_{\sigma\alpha}^{-1} - G_{\sigma\sigma}^{-1} \frac{1}{G_{\alpha\alpha}^{-1}} G_{\alpha\sigma}^{-1} \right]^{-1}, \\ G_{\sigma\alpha} &= -\frac{1}{G_{\sigma\sigma}^{-1}} G_{\sigma\alpha}^{-1} G_{\alpha\alpha} = \left[G_{\alpha\sigma}^{-1} - G_{\alpha\alpha}^{-1} \frac{1}{G_{\sigma\sigma}^{-1}} G_{\sigma\alpha}^{-1} \right]^{-1}. \end{aligned} \quad (\text{A10})$$

The second equalities in the last two equations follow by inserting the explicit expressions for $G_{\sigma\sigma}$ and $G_{\alpha\alpha}$ from the first two equations. If we assume that $\Pi_{\sigma\alpha} = \Pi_{\alpha\sigma}$, then Eq. (A6) implies that $G_{\sigma\alpha}^{-1} = G_{\alpha\sigma}^{-1}$ at the stationary point of V_{eff} . Since $G_{\sigma\sigma}^{-1}$ and $G_{\alpha\alpha}^{-1}$ are purely numbers, from the last two equations (A10) we then obtain $G_{\sigma\alpha} = G_{\alpha\sigma}$. On the other hand, if we assume the latter, then, from Eqs. (A10), we conclude that $G_{\sigma\alpha}^{-1} = G_{\alpha\sigma}^{-1}$, from which we immediately conclude via Eq. (A6) that $\Pi_{\sigma\alpha} = \Pi_{\alpha\sigma}$. In the following, we will therefore make frequent use of the symmetry property $G_{\sigma\alpha} = G_{\alpha\sigma}$.

With the explicit form (A10), we can rewrite the one-loop terms in the effective potential (A2). For the first term we obtain

$$\begin{aligned} \text{Tr} \ln G^{-1} &\equiv \ln \det G^{-1} = \ln \det \begin{pmatrix} G_{\alpha\alpha}^{-1} & G_{\alpha\sigma}^{-1} \\ G_{\sigma\alpha}^{-1} & G_{\sigma\sigma}^{-1} \end{pmatrix} + (N-1) \ln G_{\pi\pi}^{-1} \\ &= \ln [G_{\alpha\alpha}^{-1} G_{\sigma\sigma}^{-1} - G_{\alpha\sigma}^{-1} G_{\sigma\alpha}^{-1}] + (N-1) \ln G_{\pi\pi}^{-1} \\ &= \ln G_{\alpha\alpha}^{-1} + \ln \left[G_{\sigma\sigma}^{-1} - \frac{1}{G_{\alpha\alpha}^{-1}} G_{\alpha\sigma}^{-1} G_{\sigma\alpha}^{-1} \right] + (N-1) \ln G_{\pi\pi}^{-1} \\ &= \ln G_{\alpha\alpha}^{-1} + \ln [G_{\sigma\sigma}]^{-1} + (N-1) \ln G_{\pi\pi}^{-1}, \end{aligned} \quad (\text{A11})$$

where the last equality follows from comparison with the second equation (A10). Note that $[G_{\sigma\sigma}]^{-1} = G_{\sigma\sigma}^{-1} - G_{\alpha\sigma}^{-1} G_{\sigma\alpha}^{-1} / G_{\alpha\alpha}^{-1} \neq G_{\sigma\sigma}^{-1}$. To make the notation unambiguous, we put brackets around $G_{\sigma\sigma}$ before inversion. For the second one-loop term we compute with the help of Eqs. (A1) and (A8)

$$\text{Tr} [D^{-1}G] = D_{\alpha\alpha}^{-1} G_{\alpha\alpha} + D_{\alpha\sigma}^{-1} G_{\sigma\alpha} + D_{\sigma\alpha}^{-1} G_{\alpha\sigma} + D_{\sigma\sigma}^{-1} G_{\sigma\sigma} + (N-1) D_{\pi\pi}^{-1} G_{\pi\pi}. \quad (\text{A12})$$

Inserting Eqs. (A11) and (A12) into Eq. (A2), we obtain

$$\begin{aligned} V_{\text{eff}}(\phi, \alpha_0, G) &= U(\phi, \alpha_0) + \frac{1}{2} \int_K [\ln G_{\alpha\alpha}^{-1}(K) + \ln [G_{\sigma\sigma}(K)]^{-1} + (N-1) \ln G_{\pi\pi}^{-1}(K)] \\ &\quad + \frac{1}{2} \int_K [D_{\alpha\alpha}^{-1} G_{\alpha\alpha}(K) + D_{\alpha\sigma}^{-1}(\phi) G_{\sigma\alpha}(K) + D_{\sigma\alpha}^{-1}(\phi) G_{\alpha\sigma}(K) + D_{\sigma\sigma}^{-1}(K; \alpha_0) G_{\sigma\sigma}(K) \\ &\quad + (N-1) D_{\pi\pi}^{-1}(K; \alpha_0) G_{\pi\pi}(K) - (N+1)] + V_2(G). \end{aligned} \quad (\text{A13})$$

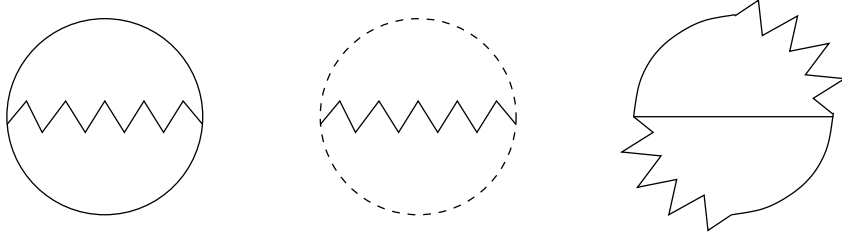


FIG. 9: Two-particle irreducible diagrams constructed from the three-point vertices in Eq. (11). The full line represents the σ field, the dashed line represents the π field and the zigzag line represents the α field. The non-diagonal propagators $G_{\alpha\sigma}$ and $G_{\sigma\alpha}$ are denoted by partially full and partially zig-zagged lines.

3. One-loop approximation

In one-loop approximation, $V_2(G) \equiv 0$, Eqs. (A4) and (A5) for the condensates ϕ and α_0 remain unchanged. For vanishing $V_2(G)$ the 1PI self-energy is equal to zero, $\Pi_{ji}(K) = 0$, and

$$G_{ji}^{-1}(K) = D_{ji}^{-1}(K; \phi, \alpha_0), \quad i, j = \alpha, \sigma, \pi_1, \dots, \pi_{N-1}. \quad (\text{A14})$$

The full two-point functions (A10) then become

$$\begin{aligned} G_{\sigma\sigma}(K) &= \left[D_{\sigma\sigma}^{-1}(K; \alpha_0) - \frac{D_{\sigma\alpha}^{-1}(\phi)D_{\alpha\sigma}^{-1}(\phi)}{D_{\alpha\alpha}^{-1}} \right]^{-1} = \left(-K^2 + i\alpha_0 + \frac{4\phi^2}{N\varepsilon} \right)^{-1}, \\ G_{\alpha\alpha}(K) &= \left[D_{\alpha\alpha}^{-1} - \frac{D_{\alpha\sigma}^{-1}(\phi)D_{\sigma\alpha}^{-1}(\phi)}{D_{\sigma\sigma}^{-1}(K; \alpha_0)} \right]^{-1} = \left(\frac{N\varepsilon}{4} + \frac{\phi^2}{-K^2 + i\alpha_0} \right)^{-1} = \frac{4}{N\varepsilon} \left[1 - \frac{4\phi^2}{N\varepsilon} G_{\sigma\sigma}(K) \right], \\ G_{\alpha\sigma}(K) &= -\frac{4i\phi}{N\varepsilon} G_{\sigma\sigma}(K) \equiv G_{\sigma\alpha}(K), \end{aligned} \quad (\text{A15})$$

where the symmetry of the mixed two-point function, $G_{\sigma\alpha} = G_{\alpha\sigma}$ is automatic. The two-point function for the pion simply reads

$$G_{\pi\pi}(K) = (-K^2 + i\alpha_0)^{-1}. \quad (\text{A16})$$

The σ and pion two-point functions can be written in the form

$$G_{\sigma\sigma}(K) = (-K^2 + M_\sigma^2)^{-1}, \quad G_{\pi\pi}(K) = (-K^2 + M_\pi^2)^{-1}, \quad (\text{A17})$$

with the same mass parameters as in Eqs. (24) and (25), since the condensate equation (A5) for α_0 is identical to the one in the shifted case, Eq. (19).

Substituting $i\alpha_0$ by Eq. (A5), the condensate equation (A4) becomes

$$h = i\alpha_0\phi + \frac{4\phi}{N\varepsilon} \int_K G_{\sigma\sigma}(K) = \frac{2\phi}{N\varepsilon} \left[\phi^2 - v_0^2 + 3 \int_K G_{\sigma\sigma}(K) + (N-1) \int_K G_{\pi\pi}(K) \right], \quad (\text{A18})$$

where we have used Eq. (A15) to rewrite $G_{\alpha\sigma}$ and $G_{\sigma\alpha}$ in terms of $G_{\sigma\sigma}$. Since $G_\sigma = G_{\sigma\sigma}$ and $G_\pi = G_{\pi\pi}$, this equation is identical with the condensate equation for ϕ in the shifted case, Eq. (22). We have therefore proved that the equations for M_σ and M_π and the condensate equation for ϕ are identical to the corresponding equations in the shifted case (ii).

4. Two-loop approximation

In case (i), to two-loop order there are only the three diagrams of sunset topology shown in Fig. 9, resulting in

$$V_2(G) = \frac{1}{4} \int_K \int_P \{ G_{\alpha\alpha}(K+P) [G_{\sigma\sigma}(K)G_{\sigma\sigma}(P) + (N-1)G_{\pi\pi}(K)G_{\pi\pi}(P)] + 2G_{\sigma\sigma}(K+P)G_{\alpha\sigma}(K)G_{\sigma\alpha}(P) \}. \quad (\text{A19})$$

Due to the absence of a four-point vertex, there is no two-loop diagram of double-bubble topology. Comparing Fig. 9 to Fig. 1, we notice that there is an additional diagram due to the presence of non-diagonal propagators, but that the last two diagrams in Fig. 1 are absent, since there is no vertex proportional to ϕ .

The equations for the two condensates ϕ and α_0 are again given by Eqs. (A4) and (A5). From Eq. (A7) we immediately derive the self-energies

$$\begin{aligned}
\Pi_{\alpha\alpha}(K) &= \frac{1}{2} \int_P [G_{\sigma\sigma}(P)G_{\sigma\sigma}(K-P) + (N-1)G_{\pi\pi}(P)G_{\pi\pi}(K-P)] , \\
\Pi_{\sigma\alpha}(K) &= \int_P G_{\sigma\alpha}(P)G_{\sigma\sigma}(K-P) , \\
\Pi_{\alpha\sigma}(K) &= \int_P G_{\alpha\sigma}(P)G_{\sigma\sigma}(K-P) , \\
\Pi_{\sigma\sigma}(K) &= \int_P [G_{\sigma\sigma}(P)G_{\alpha\alpha}(K-P) + G_{\alpha\sigma}(P)G_{\sigma\alpha}(K-P)] , \\
\Pi_{\pi\pi}(K) &= \int_P G_{\pi\pi}(P)G_{\alpha\alpha}(K-P) .
\end{aligned} \tag{A20}$$

Since $G_{\alpha\sigma} = G_{\sigma\alpha}$ at the stationary point, we confirm that $\Pi_{\alpha\sigma} = \Pi_{\sigma\alpha}$.

Replacing α_0 by Eq. (A5) the equation for the condensate ϕ reads

$$h = \frac{2\phi}{N\varepsilon} \left[\phi^2 - v_0^2 + \int_K G_{\sigma\sigma}(K) + (N-1) \int_K G_{\pi\pi}(K) \right] + \frac{i}{2} \int_K [G_{\sigma\alpha}(K) + G_{\alpha\sigma}(K)] . \tag{A21}$$

After substituting α_0 by Eq. (A5) the Dyson equations for the full two-point functions are given by

$$G_{\alpha\alpha}^{-1}(K) = D_{\alpha\alpha}^{-1} + \Pi_{\alpha\alpha}(K) = \frac{N\varepsilon}{4} + \frac{1}{2} \int_P [G_{\sigma\sigma}(P)G_{\sigma\sigma}(K-P) + (N-1)G_{\pi\pi}(P)G_{\pi\pi}(K-P)] , \tag{A22}$$

$$G_{\sigma\alpha}^{-1}(K) = D_{\sigma\alpha}^{-1}(\phi) + \Pi_{\sigma\alpha}(K) = i\phi + \int_P G_{\sigma\alpha}(P)G_{\sigma\sigma}(K-P) , \tag{A23}$$

$$G_{\alpha\sigma}^{-1}(K) = D_{\alpha\sigma}^{-1}(\phi) + \Pi_{\alpha\sigma}(K) = i\phi + \int_P G_{\alpha\sigma}(P)G_{\sigma\sigma}(K-P) , \tag{A24}$$

$$\begin{aligned}
G_{\sigma\sigma}^{-1}(K) &= D_{\sigma\sigma}^{-1}(K; \alpha_0) + \Pi_{\sigma\sigma}(K) = -K^2 + i\alpha_0 + \int_P [G_{\sigma\sigma}(P)G_{\alpha\alpha}(K-P) + G_{\alpha\sigma}(P)G_{\sigma\alpha}(K-P)] \\
&= -K^2 + \frac{2}{N\varepsilon} \left[\phi^2 - v_0^2 + \int_K G_{\sigma\sigma}(K) + (N-1) \int_K G_{\pi\pi}(K) \right] \\
&\quad + \int_P [G_{\sigma\sigma}(P)G_{\alpha\alpha}(K-P) + G_{\alpha\sigma}(P)G_{\sigma\alpha}(K-P)] ,
\end{aligned} \tag{A25}$$

$$\begin{aligned}
G_{\pi\pi}^{-1}(K) &= D_{\pi\pi}^{-1}(K; \alpha_0) + \Pi_{\pi\pi}(K) = -K^2 + i\alpha_0 + \int_P G_{\pi\pi}(P)G_{\alpha\alpha}(K-P) \\
&= -K^2 + \frac{2}{N\varepsilon} \left[\phi^2 - v_0^2 + \int_K G_{\sigma\sigma}(K) + (N-1) \int_K G_{\pi\pi}(K) \right] + \int_P G_{\pi\pi}(P)G_{\alpha\alpha}(K-P) .
\end{aligned} \tag{A26}$$

5. Recovering the standard two-loop approximation

In this subsection, we show that, up to two-loop order, the condensate and mass equations, the full propagators, as well as the effective potential become identical with the corresponding quantities for the standard linear σ model, once we eliminate the α field using the condensate equation (A5), as well as the corresponding propagators at their stationary values, cf. Eqs. (A22) – (A24).

We first consider Eq. (A21). The α_0 field has already been substituted, and we just have to replace $G_{\sigma\alpha}$ and $G_{\alpha\sigma}$ by their stationary values. To this end, we use $G_{\sigma\alpha} = G_{\alpha\sigma}$ and the third Eq. (A10), where we substitute $G_{\alpha\alpha}^{-1}$ and $G_{\alpha\sigma}^{-1}$ from Eqs. (A22) and (A24). Then, expanding to two-loop order (i.e., retaining only terms of first order in the

self-energies $\Pi_{\alpha\alpha}$ and $\Pi_{\alpha\sigma}$),

$$\begin{aligned}
\frac{1}{2} [G_{\sigma\alpha}(K) + G_{\alpha\sigma}(K)] &= G_{\alpha\sigma}(K) = - [D_{\alpha\alpha}^{-1} + \Pi_{\alpha\alpha}(K)]^{-1} [D_{\alpha\sigma}^{-1}(\phi) + \Pi_{\alpha\sigma}(K)] G_{\sigma\sigma}(K) \\
&\simeq -D_{\alpha\alpha} [D_{\alpha\sigma}^{-1}(\phi) + \Pi_{\alpha\sigma}(K) - D_{\alpha\alpha} \Pi_{\alpha\alpha}(K) D_{\alpha\sigma}^{-1}(\phi)] G_{\sigma\sigma}(K) \\
&= -\frac{4i\phi}{N\varepsilon} G_{\sigma\sigma}(K) - \frac{4}{N\varepsilon} \int_P G_{\alpha\sigma}(P) G_{\sigma\sigma}(K-P) \\
&\quad + \frac{i\phi}{2} \left(\frac{4}{N\varepsilon} \right)^2 \int_P [G_{\sigma\sigma}(P) G_{\sigma\sigma}(K-P) + (N-1) G_{\pi\pi}(P) G_{\pi\pi}(K-P)] . \tag{A27}
\end{aligned}$$

To two-loop order, we may then replace $G_{\alpha\sigma}(P)$ under the integral by the first-order contribution $-4i\phi/(N\varepsilon) G_{\sigma\sigma}(P)$. Inserting everything into Eq. (A21), we obtain Eq. (30).

Let us now consider the full propagators $G_{\sigma\sigma}$ and $G_{\pi\pi}$. Since we are working at two-loop order in the effective potential, it is sufficient to compute these propagators to one-loop order, i.e., by considering terms up to linear order in the self-energies $\Pi_{ij}(K)$. Thus, using the stationary values (A22) – (A25) we may expand the (inverse of the) second Eq. (A10) as

$$\begin{aligned}
[G_{\sigma\sigma}(K)]^{-1} &= G_{\sigma\sigma}^{-1}(K) - G_{\sigma\alpha}^{-1}(K) \frac{1}{G_{\alpha\alpha}^{-1}(K)} G_{\alpha\sigma}^{-1}(K) \\
&= D_{\sigma\sigma}^{-1}(K; \alpha_0) + \Pi_{\sigma\sigma}(K) - [D_{\sigma\alpha}^{-1}(\phi) + \Pi_{\sigma\alpha}(K)] [D_{\alpha\alpha}^{-1} + \Pi_{\alpha\alpha}(K)]^{-1} [D_{\alpha\sigma}^{-1}(\phi) + \Pi_{\alpha\sigma}(K)] \\
&\simeq D_{\sigma\sigma}^{-1}(K; \alpha_0) - D_{\alpha\alpha} D_{\sigma\alpha}^{-2}(\phi) + \Pi_{\sigma\sigma}(K) + D_{\alpha\alpha}^2 D_{\sigma\alpha}^{-2}(\phi) \Pi_{\alpha\alpha}(K) - 2 D_{\alpha\alpha} D_{\alpha\sigma}^{-1}(\phi) \Pi_{\sigma\alpha}(K) , \tag{A28}
\end{aligned}$$

where we have used $D_{\alpha\sigma}^{-1}(\phi) = D_{\sigma\alpha}^{-1}(\phi)$ and $\Pi_{\alpha\sigma}(K) = \Pi_{\sigma\alpha}(K)$. The first two terms are identical with the tree-level propagator in the shifted case,

$$D_{\sigma\sigma}^{-1}(K; \alpha_0) - D_{\alpha\alpha} D_{\sigma\alpha}^{-2}(\phi) = -K^2 + i\alpha_0 + \frac{4\phi^2}{N\varepsilon} \equiv \bar{D}_\sigma^{-1}(K; \phi, \alpha_0) , \tag{A29}$$

cf. Eq. (15). Inserting Eq. (A5), this can be written as

$$\bar{D}_\sigma^{-1}(K; \phi, \alpha_0) = -K^2 + \frac{2}{N\varepsilon} \left[3\phi^2 - v_0^2 + \int_K G_{\sigma\sigma}(K) + (N-1) \int_K G_{\pi\pi}(K) \right] . \tag{A30}$$

To one-loop order, i.e., employing the one-loop results (A15) for the propagators involving the α field, the remaining terms in Eq. (A28) can be written as

$$\begin{aligned}
&\Pi_{\sigma\sigma}(K) + D_{\alpha\alpha}^2 D_{\sigma\alpha}^{-2}(\phi) \Pi_{\alpha\alpha}(K) - 2 D_{\alpha\alpha} D_{\alpha\sigma}^{-1}(\phi) \Pi_{\sigma\alpha}(K) \\
&= \int_P \left\{ G_{\sigma\sigma}(P) G_{\alpha\alpha}(K-P) + G_{\alpha\sigma}(P) G_{\sigma\alpha}(K-P) \right. \\
&\quad \left. - \frac{1}{2} \left(\frac{4\phi}{N\varepsilon} \right)^2 [G_{\sigma\sigma}(P) G_{\sigma\sigma}(K-P) + (N-1) G_{\pi\pi}(P) G_{\pi\pi}(K-P)] - 2i \frac{4\phi}{N\varepsilon} G_{\sigma\alpha}(P) G_{\sigma\sigma}(K-P) \right\} \\
&\simeq \int_P \left\{ \frac{4}{N\varepsilon} G_{\sigma\sigma}(P) \left[1 - \frac{4\phi^2}{N\varepsilon} G_{\sigma\sigma}(K-P) \right] - \left(\frac{4\phi}{N\varepsilon} \right)^2 G_{\sigma\sigma}(P) G_{\sigma\sigma}(K-P) \right. \\
&\quad \left. - \frac{1}{2} \left(\frac{4\phi}{N\varepsilon} \right)^2 [G_{\sigma\sigma}(P) G_{\sigma\sigma}(K-P) + (N-1) G_{\pi\pi}(P) G_{\pi\pi}(K-P)] - 2 \left(\frac{4\phi}{N\varepsilon} \right)^2 G_{\sigma\sigma}(P) G_{\sigma\sigma}(K-P) \right\} \\
&= \frac{4}{N\varepsilon} \int_P G_{\sigma\sigma}(P) - 2 \left(\frac{2\phi}{N\varepsilon} \right)^2 \int_P [9 G_{\sigma\sigma}(P) G_{\sigma\sigma}(K-P) + (N-1) G_{\pi\pi}(P) G_{\pi\pi}(K-P)] . \tag{A31}
\end{aligned}$$

Summing Eqs. (A30) and (A31), we see that $[G_{\sigma\sigma}(K)]^{-1}$ becomes identical to the full inverse σ propagator in the standard $O(N)$ linear σ model, cf. Eq. (43). For the inverse pion propagator (A26), we simply have to insert the

one-loop result (A15) for $G_{\alpha\alpha}(K - P)$ in the last term,

$$\begin{aligned}
G_{\pi\pi}^{-1}(K) &= -K^2 + \frac{2}{N\varepsilon} \left[\phi^2 - v_0^2 + \int_K G_{\sigma\sigma}(K) + (N-1) \int_K G_{\pi\pi}(K) \right] + \int_P G_{\pi\pi}(P) G_{\alpha\alpha}(K - P) \\
&\simeq -K^2 + \frac{2}{N\varepsilon} \left\{ \phi^2 - v_0^2 + \int_K G_{\sigma\sigma}(K) + (N-1) \int_K G_{\pi\pi}(K) + 2 \int_P G_{\pi\pi}(P) \left[1 - \frac{4\phi^2}{N\varepsilon} G_{\sigma\sigma}(K - P) \right] \right\} \\
&= -K^2 + \frac{2}{N\varepsilon} \left\{ \phi^2 - v_0^2 + \int_K G_{\sigma\sigma}(K) + (N+1) \int_K G_{\pi\pi}(K) - \frac{8\phi^2}{N\varepsilon} \int_P G_{\pi\pi}(P) G_{\sigma\sigma}(K - P) \right\}. \quad (\text{A32})
\end{aligned}$$

This is identical with the inverse pion propagator (44) in the standard linear σ model.

Finally, we show that the two-loop effective potential (A13) becomes identical with the one for the standard linear σ model, Eq. (39), if we replace the expectation value and the full two-point function for the auxiliary field by their stationary values. We again consider the tree-level, the one-loop, and the two-loop contributions in Eq. (16) separately. Since the condensate equation for α_0 is the same in both cases, cf. Eqs. (19) and (A5), the tree-level potential at the stationary value for α_0 is given by the same expression as in the shifted case (ii), cf. Eq. (47).

For the one-loop terms, we first prove that, up to two-loop order, the following identity holds,

$$\ln G_{\alpha\alpha}^{-1} + D_{\alpha\alpha}^{-1} G_{\alpha\alpha} + D_{\alpha\sigma}^{-1} G_{\sigma\alpha} + D_{\sigma\alpha}^{-1} G_{\alpha\sigma} + D_{\sigma\sigma}^{-1} G_{\sigma\sigma} \simeq 1 + \left(D_{\sigma\sigma}^{-1} - D_{\sigma\alpha}^{-1} \frac{1}{D_{\alpha\alpha}^{-1}} D_{\alpha\sigma}^{-1} \right) G_{\sigma\sigma} + \text{const.}, \quad (\text{A33})$$

where the last term is a(n irrelevant) constant. Inserting the formal solutions (A10) for $G_{\sigma\alpha}$ and $G_{\alpha\sigma}$, the left-hand side of Eq. (A33) can be written as

$$\ln(D_{\alpha\alpha}^{-1} + \Pi_{\alpha\alpha}) + \left(D_{\alpha\alpha}^{-1} - D_{\alpha\sigma}^{-1} G_{\sigma\alpha}^{-1} \frac{1}{G_{\sigma\sigma}^{-1}} \right) G_{\alpha\alpha} + \left(D_{\sigma\sigma}^{-1} - D_{\sigma\alpha}^{-1} G_{\alpha\sigma}^{-1} \frac{1}{G_{\alpha\alpha}^{-1}} \right) G_{\sigma\sigma} \quad (\text{A34})$$

Up to two-loop order, it is sufficient to expand the first term up to first order in $\Pi_{\alpha\alpha}$,

$$\ln(D_{\alpha\alpha}^{-1} + \Pi_{\alpha\alpha}) \simeq \ln D_{\alpha\alpha}^{-1} + D_{\alpha\alpha} \Pi_{\alpha\alpha}. \quad (\text{A35})$$

Since $\ln D_{\alpha\alpha}^{-1} = \ln N\varepsilon/4$ is an irrelevant constant, we only need to retain the second term. Using the Dyson equation (A24) we may then rewrite the left-hand side of Eq. (A33) as

$$\begin{aligned}
&D_{\alpha\alpha} \Pi_{\alpha\alpha} + \left[D_{\alpha\alpha}^{-1} - (G_{\alpha\sigma}^{-1} - \Pi_{\alpha\sigma}) G_{\sigma\alpha}^{-1} \frac{1}{G_{\sigma\sigma}^{-1}} \right] G_{\alpha\alpha} + \left[D_{\sigma\sigma}^{-1} - D_{\sigma\alpha}^{-1} (D_{\alpha\sigma}^{-1} + \Pi_{\alpha\sigma}) \frac{1}{G_{\alpha\alpha}^{-1}} \right] G_{\sigma\sigma} \\
&\simeq D_{\alpha\alpha} \Pi_{\alpha\alpha} + \left(G_{\alpha\alpha}^{-1} - \Pi_{\alpha\alpha} - G_{\alpha\sigma}^{-1} G_{\sigma\alpha}^{-1} \frac{1}{G_{\sigma\sigma}^{-1}} + \Pi_{\alpha\sigma} G_{\sigma\alpha}^{-1} \frac{1}{G_{\sigma\sigma}^{-1}} \right) G_{\alpha\alpha} \\
&+ \left[D_{\sigma\sigma}^{-1} - D_{\sigma\alpha}^{-1} (D_{\alpha\sigma}^{-1} + \Pi_{\alpha\sigma}) \frac{1}{D_{\alpha\alpha}^{-1}} (1 - D_{\alpha\alpha} \Pi_{\alpha\alpha}) \right] G_{\sigma\sigma}, \quad (\text{A36})
\end{aligned}$$

where we have used Eq. (A22) and again expanded up to first order in $\Pi_{\alpha\alpha}$. The first and the third term in the first parentheses yield $[G_{\alpha\alpha}]^{-1}$, cf. the first Eq. (A10). To two-loop order, the terms in brackets may be expanded to first order in the self-energies Π_{ij} . We then obtain

$$D_{\alpha\alpha} \Pi_{\alpha\alpha} + 1 - \left(\Pi_{\alpha\alpha} - \Pi_{\alpha\sigma} \frac{G_{\sigma\alpha}^{-1}}{G_{\sigma\sigma}^{-1}} \right) G_{\alpha\alpha} + \left(D_{\sigma\sigma}^{-1} - \frac{D_{\sigma\alpha}^{-1} D_{\alpha\sigma}^{-1}}{D_{\alpha\alpha}^{-1}} - \frac{D_{\sigma\alpha}^{-1}}{D_{\alpha\alpha}^{-1}} \Pi_{\alpha\sigma} + D_{\sigma\alpha}^{-1} D_{\alpha\sigma}^{-1} D_{\alpha\alpha}^2 \Pi_{\alpha\alpha} \right) G_{\sigma\sigma}. \quad (\text{A37})$$

The second term and the two first terms in the second set of parentheses already yield the right-hand side of Eq. (A33). We thus have to show that the remaining terms cancel up to the order we are computing.

Let us first look at the second term in the first, and the third term in the second parentheses,

$$\Pi_{\alpha\sigma} \frac{G_{\sigma\alpha}^{-1}}{G_{\sigma\sigma}^{-1}} G_{\alpha\alpha} - \frac{D_{\sigma\alpha}^{-1}}{D_{\alpha\alpha}^{-1}} \Pi_{\alpha\sigma} G_{\sigma\sigma} = \Pi_{\alpha\sigma} \left(\frac{G_{\sigma\alpha}^{-1}}{G_{\alpha\alpha}^{-1}} - \frac{D_{\sigma\alpha}^{-1}}{D_{\alpha\alpha}^{-1}} \right) G_{\sigma\sigma}, \quad (\text{A38})$$

where we have used Eq. (A10) to replace $G_{\alpha\alpha}/G_{\sigma\sigma}^{-1}$ by $G_{\sigma\sigma}/G_{\alpha\alpha}^{-1}$. To two-loop order, we may now safely approximate $G_{\sigma\alpha}^{-1}/G_{\alpha\alpha}^{-1}$ by $D_{\sigma\alpha}^{-1}/D_{\alpha\alpha}^{-1}$, and we see that the expression (A38) vanishes. The remaining terms in Eq. (A37), which we have to consider, are

$$(D_{\alpha\alpha} - G_{\alpha\alpha} + D_{\sigma\alpha}^{-1} D_{\alpha\sigma}^{-1} D_{\alpha\alpha}^2 G_{\sigma\sigma}) \Pi_{\alpha\alpha}. \quad (\text{A39})$$

To two-loop order, we may replace

$$\frac{D_{\sigma\alpha}^{-1}D_{\alpha\sigma}^{-1}}{D_{\alpha\alpha}^{-1}} \simeq \frac{G_{\sigma\alpha}^{-1}G_{\alpha\sigma}^{-1}}{G_{\alpha\alpha}^{-1}} \equiv G_{\sigma\sigma}^{-1} - [G_{\sigma\sigma}]^{-1} , \quad (\text{A40})$$

where we have used the (inverse of the) second Eq. (A10). Inserting this into Eq. (A39), we obtain

$$\begin{aligned} (D_{\alpha\alpha} - G_{\alpha\alpha} + D_{\sigma\alpha}^{-1}D_{\alpha\sigma}^{-1}D_{\alpha\alpha}^2 G_{\sigma\sigma}) \Pi_{\alpha\alpha} &\simeq (D_{\alpha\alpha} - G_{\alpha\alpha} + D_{\alpha\alpha} \{G_{\sigma\sigma}^{-1} - [G_{\sigma\sigma}]^{-1}\} G_{\sigma\sigma}) \Pi_{\alpha\alpha} \\ &= \left(-G_{\alpha\alpha} + \frac{G_{\sigma\sigma}^{-1}}{D_{\alpha\alpha}^{-1}} G_{\sigma\sigma} \right) \Pi_{\alpha\alpha} \simeq \left(-G_{\alpha\alpha} + \frac{G_{\sigma\sigma}^{-1}}{G_{\alpha\alpha}^{-1}} G_{\sigma\sigma} \right) \Pi_{\alpha\alpha} , \end{aligned} \quad (\text{A41})$$

where we have again made use of $D_{\alpha\alpha}^{-1} \simeq G_{\alpha\alpha}^{-1}$ (which is correct up to the order we are computing). The right-hand side of this equation vanishes on account of the first two Eqs. (A10). We have thus proved the validity of Eq. (A33) up to two-loop order.

All one-loop terms in Eq. (A13) can now be written as

$$\begin{aligned} &\frac{1}{2} \int_K [\ln G_{\alpha\alpha}^{-1}(K) + \ln [G_{\sigma\sigma}(K)]^{-1} + (N-1) \ln G_{\pi\pi}^{-1}(K) \\ &+ D_{\alpha\alpha}^{-1} G_{\alpha\alpha}(K) + D_{\alpha\sigma}^{-1}(\phi) G_{\sigma\alpha}(K) + D_{\sigma\alpha}^{-1}(\phi) G_{\alpha\sigma}(K) + D_{\sigma\sigma}^{-1}(K; \alpha_0) G_{\sigma\sigma}(K) + (N-1) D_{\pi\pi}^{-1}(K; \alpha_0) G_{\pi\pi}(K) - (N+1)] \\ &\simeq \frac{1}{2} \int_K \left\{ \ln [G_{\sigma\sigma}(K)]^{-1} + (N-1) \ln G_{\pi\pi}^{-1}(K) \right. \\ &\quad \left. + \left[D_{\sigma\sigma}^{-1}(K; \alpha_0) - \frac{D_{\sigma\alpha}^{-1}(\phi) D_{\alpha\sigma}^{-1}(\phi)}{D_{\alpha\alpha}^{-1}} \right] G_{\sigma\sigma}(K) + (N-1) D_{\pi\pi}^{-1}(K; \alpha_0) G_{\pi\pi}(K) - N \right\} \\ &= \frac{1}{2} \int_K \left\{ \ln [G_{\sigma\sigma}(K)]^{-1} + (N-1) \ln G_{\pi\pi}^{-1}(K) \right. \\ &\quad \left. + \left[-K^2 + \frac{2}{N\varepsilon} (3\phi^2 - v_0^2) \right] G_{\sigma\sigma}(K) + (N-1) \left[-K^2 + \frac{2}{N\varepsilon} (\phi^2 - v_0^2) \right] G_{\pi\pi}(K) - N \right\} \\ &+ \frac{2}{N\varepsilon} \left\{ \int_K [G_{\sigma\sigma}(K) + (N-1) G_{\pi\pi}(K)] \right\}^2 . \end{aligned} \quad (\text{A42})$$

Finally, we consider $V_2(G)$, cf. Eq. (A19), for the stationary values of the two-point functions involving the α field. To two-loop order, it is sufficient to replace all these functions by the corresponding expressions given in Eq. (A15), resulting in

$$\begin{aligned} V_2(G) &\simeq \frac{1}{N\varepsilon} \left[\int_K G_{\sigma\sigma}(K) \right]^2 + \frac{N-1}{N\varepsilon} \left[\int_K G_{\pi\pi}(K) \right]^2 \\ &\quad - \left(\frac{2\phi}{N\varepsilon} \right)^2 \int_K \int_P G_{\sigma}(K+P) [3G_{\sigma}(K)G_{\sigma}(P) + (N-1)G_{\pi}(K)G_{\pi}(P)] . \end{aligned} \quad (\text{A43})$$

Adding Eqs. (47), (A42), and (A43), we see that the effective potential becomes identical to the one in the standard linear σ model, Eq. (39).

Appendix B: Renormalization

In this appendix, we demonstrate how to renormalize our linear σ model within the auxiliary-field method in one-loop approximation. There is a rich literature on this subject: the renormalization of scalar field theories within Φ -derivable approximation schemes was, to our knowledge for the first time, demonstrated in Ref. [39]. An iterative renormalization scheme for the $O(N)$ model in the $1/N$ expansion was developed in Ref. [40]. This scheme was applied to pion and kaon condensation in Ref. [41]. In Refs. [32, 33] the $O(N)$ model was renormalized using the $1/N$ expansion within the auxiliary-field method. Here, we follow Ref. [42] where a one-step approach to renormalization of Φ -derivable approximations was introduced and shown to be equivalent to the iterative renormalization scheme of the above works. We mention that this one-step approach was also used in Ref. [34] for the renormalization of the $O(N)$ model using the $1/N$ expansion both with and without the auxiliary-field method.

In order to renormalize Eqs. (22), (24), and (25) to one-loop order it is sufficient to add the following five counter terms to the tree-level potential $U(\phi, \alpha_0)$:

$$\frac{1}{2} \delta Z_1 i \alpha_0 \phi^2 - \frac{1}{2} \delta Z_2 i \alpha_0 v_0^2 + \frac{N \varepsilon}{8} \delta Z_3 \alpha^2 + \frac{\delta Z_4}{2} \phi^2 + \frac{\delta Z_5}{4} \phi^4, \quad (\text{B1})$$

such that

$$U(\phi, \alpha_0) \longrightarrow U_{CT}(\phi, \alpha_0) = \frac{i}{2} Z_1 \alpha_0 \phi^2 - \frac{i}{2} Z_2 \alpha_0 v_0^2 + \frac{N \varepsilon}{8} Z_3 \alpha^2 + \frac{\delta Z_4}{2} \phi^2 + \frac{\delta Z_5}{4} \phi^4, \quad (\text{B2})$$

where $Z_i = 1 + \delta Z_i$ $i = 1, 2, 3$. Equations (22) and (25) then read

$$h = \phi \left[Z_1 i \alpha_0 + \delta Z_4 + \delta Z_5 \phi^2 + \frac{4}{N \varepsilon} \int_K G_\sigma(K) \right], \quad (\text{B3})$$

$$M_\pi^2 = i \alpha_0 = \frac{2}{Z_3 N \varepsilon} \left[Z_1 \phi^2 - Z_2 v_0^2 + \int_K G_\sigma(K) + (N-1) \int_K G_\pi(K) \right]. \quad (\text{B4})$$

Using a cut-off Λ_{CO} for the four-dimensional momentum integration (and neglecting terms of order $\mu^2/\Lambda_{\text{CO}}^2$, where μ is the renormalization scale) the tadpole integrals can be written as [42]

$$\int_K G_i(K) = \Lambda^2 + T_d M_i^2 + T_F^i, \quad (\text{B5})$$

where $\Lambda = 4\pi\Lambda_{\text{CO}}$,

$$T_d = -\frac{1}{16\pi^2} \ln \frac{16\pi^2 \Lambda^2}{\mu^2 e},$$

and

$$T_F^i = \int \frac{d^3 \vec{k}}{(2\pi)^3} \frac{1}{\sqrt{\vec{k}^2 + M_i^2}} \left[\exp\left(\sqrt{\vec{k}^2 + M_i^2}/T\right) - 1 \right]^{-1} + \frac{1}{16\pi^2} \left(M_i^2 \ln \frac{M_i^2}{\mu^2} - M_i^2 + \mu^2 \right), \quad i = \sigma, \pi. \quad (\text{B6})$$

Inserting Eq. (B5) into Eq. (B4), we obtain

$$\begin{aligned} M_\pi^2 &= \frac{2}{N \varepsilon} \left(\frac{Z_1}{Z_3} \phi^2 - \frac{Z_2}{Z_3} v_0^2 + \frac{1}{Z_3} \left\{ N \Lambda^2 + T_F^\sigma + (N-1) T_F^\pi + \frac{2T_d}{\varepsilon} \left[\frac{N+2}{N} \phi^2 - v_0^2 + T_F^\sigma + (N-1) T_F^\pi \right] \right\} \right) \\ &= \frac{2}{N \varepsilon} [\phi^2 - v_0^2 + T_F^\sigma + (N-1) T_F^\pi] \\ &+ \frac{2}{N \varepsilon} \left\{ \left(\frac{Z_1}{Z_3} - 1 \right) \phi^2 - \left(\frac{Z_2}{Z_3} - 1 \right) v_0^2 + \frac{1}{Z_3} \left\{ N \Lambda^2 + \frac{2T_d}{\varepsilon} \left[\frac{N+2}{N} \phi^2 - v_0^2 + T_F^\sigma + (N-1) T_F^\pi \right] \right\} \right. \\ &\quad \left. + \left(\frac{1}{Z_3} - 1 \right) [T_F^\sigma + (N-1) T_F^\pi] \right\}. \end{aligned} \quad (\text{B7})$$

The first line is the expected, finite result for the pion mass (squared). The renormalization constants have to be chosen such that the second and third lines vanish. Cancellation of the temperature-dependent sub-divergence [the terms proportional to $T_F^\sigma + (N-1)T_F^\pi$] requires

$$Z_3 = 1 + \frac{2T_d}{\varepsilon} \iff \delta Z_3 = \frac{2T_d}{\varepsilon}. \quad (\text{B8})$$

Cancellation of the ϕ -dependent overall divergence gives

$$\frac{Z_1}{Z_3} - 1 = -\frac{2T_d}{\varepsilon} \frac{N+2}{N} \iff Z_1 = 1 - \frac{4T_d}{N \varepsilon} \iff \delta Z_1 = -\frac{4T_d}{N \varepsilon}, \quad (\text{B9})$$

where we have used the result (B8) for Z_3 . Finally, cancellation of the constant overall divergence yields

$$\frac{N \Lambda^2}{Z_3} = v_0^2 \left(\frac{Z_2}{Z_3} - 1 + \frac{2T_d}{\varepsilon Z_3} \right) \iff Z_2 = 1 + \frac{N \Lambda^2}{v_0^2} \iff \delta Z_2 = \frac{N \Lambda^2}{v_0^2}, \quad (\text{B10})$$

where we have again used Eq. (B8). Finally, turning to Eq. (B3), we can use $M_\pi^2 = i\alpha_0$ and Eq. (B5) to write

$$h = \phi \left[Z_1 M_\pi^2 + \delta Z_4 + \delta Z_5 \phi^2 + \frac{4}{N\varepsilon} (\Lambda^2 + T_d M_\sigma^2 + T_F^\sigma) \right]. \quad (\text{B11})$$

Using the result (B9) for Z_1 , we obtain

$$h = \phi \left[M_\pi^2 + \frac{4}{N\varepsilon} T_F^\sigma + \delta Z_4 + \frac{4\Lambda^2}{N\varepsilon} + \delta Z_5 \phi^2 + \frac{4T_d}{N\varepsilon} (M_\sigma^2 - M_\pi^2) \right]. \quad (\text{B12})$$

The first two terms represent the expected, finite result. The counter terms $\delta Z_{4,5}$ have to be chosen such that the remaining (infinite) terms cancel. Using the fact that

$$M_\sigma^2 = M_\pi^2 + \frac{4\phi^2}{N\varepsilon}, \quad (\text{B13})$$

we see that this is achieved by the choice

$$\delta Z_4 = -\frac{4\Lambda^2}{N\varepsilon}, \quad (\text{B14})$$

$$\delta Z_5 = -\frac{16T_d}{N^2\varepsilon^2}. \quad (\text{B15})$$

This completes the renormalization of the linear σ model in one-loop approximation within the auxiliary-field method.

Thus, to one-loop order the renormalized equations for the condensate and for the masses read

$$h = \frac{2\phi}{N\varepsilon} [\phi^2 - v_0^2 + 3T_F^\sigma + (N-1)T_F^\pi], \quad (\text{B16})$$

$$M_\pi^2 = \frac{2}{N\varepsilon} [\phi^2 - v_0^2 + T_F^\sigma + (N-1)T_F^\pi], \quad (\text{B17})$$

$$M_\sigma^2 = \frac{2}{N\varepsilon} [3\phi^2 - v_0^2 + T_F^\sigma + (N-1)T_F^\pi]. \quad (\text{B18})$$

where T_F^i is given by Eq. (B6).

-
- [1] G. 't Hooft, Phys. Rept. **142**, 357 (1986).
[2] C. Vafa and E. Witten, Nucl. Phys. B **234**, 173 (1984).
[3] Proc. of LATTICE '96, Nucl. Phys. B **53** (Proc. Suppl.), 1 (1997).
[4] R. D. Pisarski and F. Wilczek, Phys. Rev. D **29**, 338 (1984).
[5] L. Dolan and R. Jackiw, Phys. Rev. D **9**, 2904 (1974).
[6] E. Braaten and R. D. Pisarski, Nucl. Phys. B **337**, 569 (1990).
[7] J. M. Cornwall, R. Jackiw and E. Tomboulis, Phys. Rev. D **10**, 2428 (1974).
[8] G. Baym and L. P. Kadanoff, Phys. Rev. **124**, 287 (1961).
[9] J. M. Luttinger and J. C. Ward, Phys. Rev. **118**, 1417 (1960).
[10] G. Baym, Phys. Rev. **127**, 1391 (1962).
[11] H. van Hees and J. Knoll, Phys. Rev. D **66**, 025028 (2002).
[12] N. Petropoulos, J. Phys. G **25**, 2225 (1999).
[13] J. T. Lenaghan and D. H. Rischke, J. Phys. G **26**, 431 (2000).
[14] S. Chiku and T. Hatsuda, Phys. Rev. D **58**, 076001 (1998); S. Chiku Prog. Theor. Phys. **104**, 1129 (2000).
[15] J. T. Lenaghan, D. H. Rischke, and J. Schaffner-Bielich, Phys. Rev. D **62**, 085008 (2000) [nucl-th/0004006].
[16] D. Roder, J. Ruppert and D. H. Rischke, Phys. Rev. D **68**, 016003 (2003).
[17] G. Baym and G. Grinstein, Phys. Rev. D **15**, 2897 (1977).
[18] J. Polchinski, arXiv:hep-th/9611050.
[19] G. Amelino-Camelia and S. Y. Pi, Phys. Rev. D **47**, 2356 (1993).
[20] G. Amelino-Camelia, Phys. Lett. B **407**, 268 (1997).
[21] H. S. Roh and T. Matsui, Eur. Phys. J. A **1**, 205 (1998).
[22] Y. Nemoto, K. Naito and M. Oka, Eur. Phys. J. A **9**, 245 (2000).
[23] N. Petropoulos, arXiv:hep-ph/0402136.
[24] Yu. B. Ivanov, F. Riek and J. Knoll, Phys. Rev. D **71**, 105016 (2005); Yu. B. Ivanov, F. Riek, H. van Hees and J. Knoll, Phys. Rev. D **72**, 036008 (2005).

- [25] D. Roder, J. Ruppert, and D. H. Rischke, Nucl. Phys. A **775**, 127 (2006).
- [26] S. R. Coleman, R. Jackiw and H. D. Politzer, Phys. Rev. D **10**, 2491 (1974).
- [27] R. G. Root, Phys. Rev. D **10**, 3322 (1974).
- [28] H. Meyers-Ortmanns, H. J. Pirner and B. J. Schaefer, Phys. Lett. B **311**, 213 (1993).
- [29] A. Bochkarev and J. I. Kapusta, Phys. Rev. D **54**, 4066 (1996).
- [30] J. O. Andersen, D. Boer and H. J. Warringa, Phys. Rev. D **70**, 116007 (2004).
- [31] J. O. Andersen and T. Brauner, Phys. Rev. D **78**, 014030 (2008).
- [32] F. Cooper, J. F. Dawson and B. Mihaila, Phys. Rev. D **71**, 096003 (2005) [hep-ph/0502040].
- [33] A. Jakovac, Phys. Rev. D **78**, 085013 (2008) [arXiv:0808.1800 [hep-th]].
- [34] G. Fejos, A. Patkos and Z. Szep, Phys. Rev. D **80**, 025015 (2009) [arXiv:0902.0473 [hep-ph]].
- [35] R.J. Rivers, Path integral methods in quantum field theory (Cambridge University Press, Cambridge, 1987).
- [36] C. Amsler and N. A. Tornqvist, Phys. Rept. **389**, 61 (2004); E. Klempt and A. Zaitsev, Phys. Rept. **454**, 1 (2007); F. Giacosa, Phys. Rev. D **80**, 074028 (2009).
- [37] A. Heinz, S. Struber, F. Giacosa and D. H. Rischke, Acta Phys. Polon. Supp. **3**, 925 (2010).
- [38] S. Strueber and D. H. Rischke, Phys. Rev. D **77** (2008) 085004; D. Parganlija, F. Giacosa and D. H. Rischke, Phys. Rev. D **82** (2010) 054024; D. Parganlija, F. Giacosa and D. H. Rischke, Phys. Rev. D **82**, 054024 (2010); S. Gallas, F. Giacosa and D. H. Rischke, Phys. Rev. D **82**, 014004 (2010).
- [39] J. -P. Blaizot, E. Iancu and U. Reinosa, Nucl. Phys. A **736**, 149 (2004) [hep-ph/0312085].
- [40] J. Berges, S. Borsanyi, U. Reinosa and J. Serreau, Annals Phys. **320**, 344 (2005) [hep-ph/0503240].
- [41] J. O. Andersen, Phys. Rev. D **75**, 065011 (2007) [hep-ph/0609020].
- [42] G. Fejos, A. Patkos and Z. Szep, Nucl. Phys. A **803**, 115 (2008) [arXiv:0711.2933 [hep-ph]].